What do models tell us about water and sediment connectivity?

Jantiene E. M. Baartman, João Pedro Nunes, Rens Masselink, Frédéric Darboux, Charles Bielders, Aurore Degré, Vincent Cantreul, Olivier Cerdan, Thomas Grangeon, Peter Fiener, Florian Wilken, Marcus Schindewolf, John Wainwright

Angaben zur Veröffentlichung / Publication details:

Baartman, Jantiene E. M., João Pedro Nunes, Rens Masselink, Frédéric Darboux, Charles Bielders, Aurore Degré, Vincent Cantreul, et al. 2020. "What do models tell us about water and sediment connectivity?" *Geomorphology* 367: 107300. https://doi.org/10.1016/j.geomorph.2020.107300.

Geomorphology 367 (2020) 107300

Contents lists available at ScienceDirect

Geomorphology

journal homepage: www.elsevier.com/locate/geomorph

Invited research article

What do models tell us about water and sediment connectivity?

Jantiene E.M. Baartman [a,*], João Pedro Nunes [b], Rens Masselink [a], Frédéric Darboux [c], Charles Bielders [d], Aurore Degré [e], Vincent Cantreul [e], Olivier Cerdan [f], Thomas Grangeon [f], Peter Fiener [g], Florian Wilken [h,g], Marcus Schindewolf [i], John Wainwright [j]

[a] Soil Physics and Land Management group, Wageningen University, Wageningen, the Netherlands
[b] CE3C – Centre for Ecology, Evolution and Environmental Changes, Faculdade de Ciências, Universidade de Lisboa, 1749-016 Lisboa, Portugal
[c] Université de Lorraine, INRA, LSE, F-54000 Nancy, France
[d] Earth and Life Institute, Environmental Sciences, Université catholique de Louvain, Louvain-la-Neuve, Belgium
[e] Terra Research Centre, Gembloux Agro-Bio Tech, Liege University, Belgium
[f] Bureau de Recherches Géologique et Minières (BRGM), Orléans, France
[g] Water and Soil Resource Research, Institute for Geography, University Augsburg, Germany
[h] Soil Resources Research, Department of Environmental System Science, ETH Zuerich, Switzerland
[i] Thuringian State Institute of Agriculture, Jena, Germany
[j] Department of Geography, Durham University, Science Laboratories, South Road, Durham DH1 3LE, UK

ARTICLE INFO

Article history:
Received 22 October 2019
Received in revised form 28 May 2020
Accepted 11 June 2020
Available online 30 June 2020

Keywords:
Connectivity
Erosion models
Model comparison
Catchment

ABSTRACT

Connectivity has been embraced by the geosciences community as a useful concept to understand and describe hydrological functioning and sediment movement through catchments. Mathematical modelling has been used for decades to quantify and predict erosion and transport of sediments, e.g. in scenarios of land use change or conservation measures. Being intrigued by both models and the connectivity concept, as a group of modellers we aimed at investigating what different models could tell us about connectivity. Therefore, we evaluated the response of contrasted spatially-distributed models to landscape connectivity features and explained the differences based on different model structures. A total of 53 scenarios were built with varying field sizes and orientations, as well as the implementation of soil conservation measures. These scenarios were simulated, for two rainfall intensities, with five event- and process-based water and soil erosion models – EROSION3D, FullSWOF_2D, LandSoil, OpenLISEM and Watersed. Results showed that rainfall amount plays the most important role in determining relative export and connected area of runoff and sediment in all models, indicating that functional aspects of connectivity were more important than structural connectivity. As for the role of structural landscape elements, there was no overall agreement between models regarding the effects of field sizes, crop allocation pattern, and conservation practices; agreement was also low on the spatial patterns of connectivity. This overall disagreement between models was unexpected. The results of this exercise suggest that the correct parameterization of runoff and sediment production and of routing patterns may be an important issue. Thus, incorporating connectivity functions based on routing would help modelling forward. Our results also suggest that structural connectivity indices may not suffice to represent connectivity in this type of catchment (relatively simple and monotonous land cover), and functional connectivity indices should be applied.

1. Introduction

The extent to which system components are coupled controls the functioning and behaviour of Earth systems. For example, Fryirs (2013) proposed to use (dis)connectivity as framework to analyse spatial and temporal variation that operates within a catchment's sediment cascade. This (dis)connectivity of a system has emerged as a useful concept in geosciences over the last decades (e.g. Keesstra et al., 2018; Parsons et al., 2015; Wohl, 2017). The connectivity concept supported the understanding of water and sediment transfer within catchments (e.g. Bracken et al., 2015, 2013) and the concept has thus been embraced by the scientific community (e.g. Heckmann et al., 2018; Nunes et al., 2018). Bracken and Croke (2007) identified three major types of connectivity: (i) landscape connectivity relating to the physical (de) coupling of different landscape elements, (ii) hydrological connectivity, referring to the passage of water through the system, and (iii) sedimentological connectivity, relating to the transfer of sediment. Fryirs (2013) combined them and describes connectivity as the water-mediated

* Corresponding author at: Soil Physics and Land Management Group (SLM), Wageningen University, PO Box 47, 6700 AA Wageningen, the Netherlands.
E-mail address: jantiene.baartman@wur.nl (J.E.M. Baartman).

https://doi.org/10.1016/j.geomorph.2020.107300

transfer of sediment within different components of a sediment cascade. In line with Heckmann et al. (2018), connectivity can be defined as the degree to which a system facilitates the transfer of sediment and water. Connectivity thus reflects the continuity and strength of runoff and sediment pathways in a catchment at a given point in time (Heckmann et al., 2018). Often a distinction is being made between structural connectivity, representing the spatial configuration of system components, and functional connectivity, which is inferred from the actual transfer of water and sediment and is more dynamic than structural connectivity (e.g. Cossart and Fressard, 2017; David et al., 2014; López-Vicente et al., 2017; Reulier et al., 2019; Turnbull et al., 2008; Wainwright et al., 2011). Another distinction that can be made is between lateral (e.g. hillslope – channel) and longitudinal (e.g. along a river network) connectivity (Heckmann et al., 2018).

Within the geosciences, connectivity is being used and extended in several ways. Studies with a more conceptual focus, exploring connectivity as a framework, include Bracken et al. (2015); Brierley et al. (2006); Croke et al. (2005); Fryirs (2013); Fryirs et al. (2007); Keesstra et al. (2018); Lexartza-Artza and Wainwright (2009); Turnbull et al. (2008) and Wainwright et al. (2011). Several studies also highlight the potential of the connectivity concept to cross scales (e.g. Bracken et al., 2015; Darboux et al., 2002; Mueller et al., 2007; van der Ploeg et al., 2018): connectivity can be defined and quantified relatively easily for various subsystems, i.e. on different scales, which allows the subsequent evaluation of how the connectivity of one (sub) system can affect the (sub)system at another scale. One example given in Van der Ploeg et al. (2018) is that of semi-arid landscapes with banded vegetation patterns. At micro-scale, hydrological connectivity between top- and subsoil is low in the bare areas because of crusting, but high in the vegetated patches because of bioturbation; while at the landscape scale, hydrological and sediment connectivity is low because vegetation bands avoid larger-scale transport of water and sediment as they are being interrupted by the vegetation bands (e.g. Mora and Lázaro, 2013; Saco et al., 2007). Connectivity is also used in a land-management context (Gumiere et al., 2011; Keesstra et al., 2018; Mekonnen et al., 2016), for example the investigation of the role of humans in impacting fluvial systems (e.g. Poeppl et al., 2017), the effect of riparian vegetation on connectivity (Poeppl et al., 2012), the effect of land-use change (e.g. David et al., 2014; Follain et al., 2012; Llena et al., 2019), terracing (Calsamiglia et al., 2018), drainage density reduction and road networks (Persichillo et al., 2018) and dams (Poeppl et al., 2015) on sediment connectivity. Estrany et al. (2019) used high-resolution imagery to estimate sediment connectivity after vegetation disturbance. Furthermore, Smetanová et al. (2018) investigated the perception of stakeholders of water and sediment connectivity and found that half of the stakeholders considered connectivity management important, but that adopting connectivity into management was hindered by institutional- and policy-based management limitations, insufficient data and methods, and ineffective knowledge transfer. Connectivity has also been used to estimate qualitatively or (semi-) quantitatively (via connectivity indices) the degree of water and sediment fluxes in catchments from geographical information (see Ali and Roy (2010) and Heckmann et al. (2018) for reviews of hydrological and sediment connectivity). Briefly, the main aim of models is to quantify the complex dynamics of water and sediment redistribution within a catchment, while indices usually are a combination of several variables conceptually known to control the spatial organization and intensity of sediment fluxes in a landscape (Heckmann et al., 2018) and often are more static than models. An example of an index of connectivity that is being applied widely and modified for various applications is the Index of Connectivity (IC, Borselli et al. (2008); modified by, among others, Cavalli et al. (2013); Gay et al. (2016); López-Vicente et al. (2017); Martínez-Murillo and López-Vicente (2018)). Another series of indices of connectivity are derived from graph theory (e.g. Cossart and Fressard, 2017; Heckmann and Schwanghart, 2013; Masselink et al., 2017). This brief overview shows that connectivity has been embraced by the scientific geosciences community as a useful concept and some great progress has been made; but there is still considerable potential for the concept to be developed and applied further.

Numerical models are being used since the late 1960s to mathematically describe hydrological processes and sediment transport through catchments (e.g. Clarke, 1973; Foster and Meyer, 1975; Freeze and Harlan, 1969; Kirkby, 1971), either with the specific purpose to predict sediment yields under various conditions (e.g. climate change; Li and Fang, 2016) or to analyse processes and their interactions (e.g. Hartley and Julien, 1992; Takken et al., 2005). Many physically-based erosion and sediment transport models have been first developed in the 1990s (e.g. DE ROO et al., 1996a, 1996b; Nearing et al., 1990; Smith et al., 1995), when the hydrograph and sediment yield at the outlet was the main focus of the model and/or the sole possibility to calibrate these models (Batista et al., 2019). However, because many models were spatially explicit, predicting the spatial pattern and rates of erosion and deposition became increasingly important (Batista et al., 2019; Jetten et al., 2003; Takken et al., 1999). In line with the value of the connectivity concept, recent work has begun to stress that the connectivity of water and sediment could be more important than catchment internal erosion rates (Boardman et al., 2019): highly connected systems cause off-site impacts and societal or ecological nuisance such as muddy floods, not necessarily directly related to high erosion rates on field. Nunes et al. (2018) concluded that hydrologic and geomorphic catchment models can be substantially improved by improving the way in which models represent landscape connectivity.

The explicit simulation of connectivity processes in numerical models is still relatively limited (Keesstra et al., 2018; Mahoney et al., 2018). A brief summary of modelling approaches that capture various aspects of connectivity is given in Keesstra et al. (2018). Until now, mostly spatially-distributed erosion models are being applied and the expected connectivity patterns that emerge from the simulations are then being analysed in terms of connectivity, without parameterizing sub-grid processes (but see e.g. Mueller et al., 2007). Essentially all spatially explicit models that produce maps of overland flow and sediment redistribution can be used to infer connectivity (e.g. Liu and Fu, 2016), whether they are process-based erosion models, hydrological models (e.g. Appels et al., 2011; Yang and Chu, 2013), or landscape evolution models (e.g. Baartman et al., 2013; Coulthard and Van De Wiel, 2017; Lesschen et al., 2009). To incorporate sub-grid scale connectivity, 'effective' parameters (i.e. model parameters which are different from the equivalent measurement to account for a process which the model structure does not represent; Nunes et al., 2018) that capture the effect of connectivity at these small scales can be incorporated, e.g. for vegetation or roughness (Antoine et al., 2011). A few studies compare or couple numerical models and connectivity indices: López-Vicente et al. (2015, 2013) coupled the Revised Morgan-Morgan-Finney (RMMF) model (Morgan, 2001) and the Index of Connectivity (IC; Borselli et al., 2008). They used the IC maps as a proxy of sediment trapping effectiveness, which is then used in the RMMF model to calculate the effective runoff. Their results show that the inclusion of the IC maps was particularly useful for the linear features (drainage channels, terrace walls), with high connectivity leading to improved runoff prediction. Also, they found good agreement between the IC and RMMF models. They concluded that the application of trap effectiveness mask layers, based on connectivity, is of interest to improve predictions of distributed runoff and erosion models (López-Vicente et al., 2015). Poeppl et al. (2019) compare the GEOWEPP-C model (Renschler, 2003) and the IC. The match between the model prediction and field observations was partly confirmed and the GeoWEPP-C was capable of simulating flowpaths towards channels as well as sediment yields of contributing areas. Kalantari et al. (2019) included a sediment connectivity index that considers soil moisture in a flood probability model for road-stream intersections.

They concluded that the sediment connectivity index was one of the five main attributes important for flood probability quantification. Nunes et al. (2009) used the topographic wetness index to map hydrological and sediment connectivity due to soil saturation. Masselink et al. (2016) used existing data to assess governing factors of connectivity (topological, biological and soil), which were used in a linear model for discharge and suspended sediment yield. Their results show that the combination of biological and soil connectivity components yields highest efficiency coefficients for both runoff and sediment discharge, but they recommended to include spatial arrangement of the different features within the catchment as well as non-linear relations to improve the prediction for sediment transport. Recently, Mahoney et al. (2018) developed a catchment erosion model using probability theory for sediment connectivity, accounting for the spatial variability of sediment (dis)connectivity across the landscape using high-resolution DEMs. This seems a promising approach that potentially reduces computation time and includes various sediment transport criteria. Cossart et al. (2018) reported three case studies, combining graph theory, agent-based modelling and differential equations with connectivity, and found how anthropogenic structures affect structural connectivity. Their third case focused on process-based (or functional) connectivity and revealed a self-organised response and catchment level. These examples highlight the recent advances in the use of connectivity, in various ways, in modelling studies.

From this review, we can gather that although advances are being made to use connectivity in hydrology and soil erosion modelling, they are still limited. However, quantification of connectivity is being highlighted as a need given its relevance in geomorphic system functioning (Heckmann et al., 2018; Keesstra et al., 2018). Being intrigued by both models and the connectivity concept, as a group of modellers we wondered what different models could tell us about connectivity. Therefore, we set out to assess the response of contrasted water and soil erosion models to landscape connectivity features and explain the differences based on model structure. To achieve this objective, the effects of various combinations of rainfall and landscape patterns on water and sediment transport and connectivity were simulated by five spatially-distributed, event- and process-based models that differ in terms of their representation of processes and landscape features. We analysed connectivity of the model output in various ways; the connected area in terms of runoff and sediment and the total export of water and sediment were calculated for each model run. In addition, the IC (Borselli et al., 2008) was calculated for each scenario. In this paper, we first analyse each model's response to the connectivity scenarios in relation to its structure. In a second step, models are compared for specific scenarios that resulted in contrasting model outputs.

2. Methods

2.1. Modelling exercise design

The modelling exercise was designed to compare and analyse how different models simulate hydrological and sedimentological connectivities in a typical arable landscape of Central Europe. As the purpose was not to identify the best model, but rather to understand the effect of model structure and process representation on the emerging connectivity, this study was performed in a “semi-virtual” catchment without model validation and calibration but with realistic parameterization. For the semi-virtual catchment land-use scenarios, with varying patchiness resulting from different field sizes and orientations, linear landscape features, etc., were developed, while the topography and typical land management was taken from an existing catchment in the Belgian Loess Belt. Surface runoff and sediment transport in this semi-virtual catchment was analysed for block rain events of different recurrence intervals for central Belgium (1, 10, and 50 yrs).

2.2. Description of the models

In this study five different surface runoff and erosion models were used: EROSION3D, FullSWOF_2D, LandSoil, OpenLISEM, and Watersed (Table 1). The prerequisite to be included in this study was, that the models (i) were capable of dealing with changes in land use patterns and structures and their effect on both hydrological and sedimentological connectivities (except FullSWOF_2D), (ii) had been developed or at least tested earlier under similar conditions as those represented by the small semi-virtual agricultural catchment used in this analysis, and (iii) were well documented in the scientific literature. The description of the different models is focused on their main features, as well as the main differences between the models in addressing changes in land-use patterns, structures and management. An overview of the most important processes taken into account is given in Table 1, where also the most important references documenting model structures and model validation in similar catchments are given.

2.2.1. Representation of runoff generation and concentration

Surface runoff generation in the different models is either represented as Hortonian runoff or saturation runoff, whereas some models (e.g. Watersed, OpenLISEM) are able to simulate both processes. Differences in runoff generation process may substantially affect model reactions to changes in crop and field patterns. Runoff propagation is modelled either with full Shallow-Water equations (FullSWOF_2D), with the kinematic wave approximation (EROSION3D, OpenLISEM) or more model-specific approaches. All models are able to deal with runon infiltration which is the prerequisite to account for a more patchy land use, where some fields produce runoff while runon infiltration occurs on others. Major differences can be found regarding flow direction approaches (Table 1). Some models use multiple flow algorithms (e.g. FullSWOF_2D) while others use single flow algorithms (e.g. OpenLISEM). This should make a difference in terms of time to concentration and especially runon infiltration. Moreover, EROSION3D and LandSoil employ tillage direction to modify flow direction. Hence, the runoff concentration should also be affected by field oriented roughness in these two models.

2.2.2. Representation of soil erosion, sediment transport and deposition

Except for FullSWOF_2D all models are capable of representing soil erosion and sediment delivery (Table 1). Some models account for splash and interrill erosion, some only interrill erosion, while all models account for rill erosion. Ephemeral gullying is taken into account in two models only (LandSoil and Watersed; Table 1). Gullying especially should have a strong effect on hydrological and sedimentological connectivity. For most models, deposition is calculated depending on surface conditions and transport capacity, while LandSoil applies a pre-defined sediment concentration, based on vegetation cover, slope, etc. (Table 1). For sedimentological connectivity also substantial differences can be expected between models with single and multiple flow algorithms strongly affecting sediment settling. Different patterns of deposition can also be expected if tillage direction and oriented roughness is taken into account (EROSION 3D and LandSoil).

Another difference between the models is the time step (Table 1). While FullSWOF_2D uses a variable time step, the other models have fixed time steps ranging from 5 s (OpenLISEM) to an aggregated event time step (Watersed and LandSoil). This will substantially affect the ability of the different models to account for a dynamic change in hydrological and sedimentological connectivity during runoff events.

2.3. Study area, scenarios and input data

2.3.1. Description of the semi-virtual catchment

The catchment used in this study is a semi-virtual representation of a 124-ha catchment located in Chastre in the Belgian loess belt. The Belgian loess belt is known for high rates of soil erosion by water and frequent muddy floods (Bielders et al., 2003; Evrard et al., 2007).

Table 1
Overview of model features relevant for this study.

Model	Process representations													
	Surface runoff				Flow direction			Erosion/transport/deposition of soils/sediments						
Name (Version)	Infiltration	Type of runoff	Runon infiltration	Routing	Single/Multiple flow	Affected by tillage direction	Dynamic during modelling	Splash	Interrill	Rill	Ephemeral gullying	Sediment transport	Grain size specific	Deposition
EROSION 3D	Green-Ampt	Hortonian	Yes	Kinematic wave	Variable	Yes	Yes	Yes	Yes	Yes		Momentum-flux-approach	Yes	Surface conditions and transport capacity
FullSWOF_2D 1.07.01, (16/02/2017)	Green-Ampt	Hortonian and/or saturation	Yes	Full Shallow water equations	Multiple flow	No	Yes	No	No	No	No	No	No	No
LandSoil 3.7.1 (14/02/2011)	Data driven based on surface conditions (expert rules)	Hortonian	Yes	Modified D8 with tillage direction	Single flow	Yes	No	No	Yes	Yes	Yes	Maximum sediment concentration	No	Maximum sediment concentration depending on land use, slope etc
OpenLisem (2.01)	Green-Ampt	Hortonian and/or saturation	Yes	Kinematic wave	Single flow	No	No	Yes	Yes	Yes	No	Splash delivery function and stream power for overland flow	No	Surface conditions, transport capacity, flow width and settling velocity
Watersed (V1.0)	Data driven based on surface conditions	Hortonian and/or saturation	Yes	D8 or MFD (depending on local slope)	Variable	No	No	Yes	Yes	Yes	Yes	Local sediment concentration is transported along with runoff	No	Surface conditions and transport capacity

Model	Representing time and space		References	
Name	Spatial resolution [m]	Time step [s]	Details of model features	Testing and application
Erosion3D	1	Variable	Schmidt, 1996, 1991; von Werner, 1995	Schindewolf and Schmidt, 2012
FullSWOF_2D	1	Variable	Delestre et al., 2017	Botticelli et al., 2018; Delestre et al., 2013; Hong et al., 2016; Wittmann et al., 2017
LandSoil	1	Event	Cerdan et al., 2002b, 2002a; Govers et al., 1994; Souchere et al., 1998; Souchere et al., 2003; Ciampalini et al., 2012	Ciampalini et al., 2012; Evrard et al., 2009; Le Bissonnais et al., 2005, 1998
OpenLisem	1	Variable (user-choice), but fixed within one event (here: 5s)	Bout and Jetten, 2018; De Roo et al., 1996b, 1996a	Baartman et al., 2012; De Roo and Jetten, 1999; Grum et al., 2017; Hessel et al., 2003; Kværnø and Stolte, 2012; Starkloff et al., 2018; Takken et al., 1999
Watersed	1	Event	Cerdan et al., 2002b, 2002a; Landemaine, 2016	Landemaine, 2016

Elevation ranges between 128 and 161 m and slope gradients range between 0 and 15%, with a mean of 4% (Fig. 1). Cropland occupies 95% of the catchment, the remaining area consisting of green infrastructure, mostly along the main thalweg. This catchment was described in detail in Pineux et al. (2017) and Cantreul et al. (2018). The DEM was derived from 10-m resolution data (Service public de Wallonie, 2005), as higher-resolution data included connectivity features such as roads and ditches that were not possible to remove without adding other artefacts. These data were interpolated to 1 × 1 m resolution using the methodology of Hutchinson et al. (2011), designed to interpolate hydrologically correct DEMs by reconstructing ridges, streams and a connected drainage structure from contour lines. The resulting data were post-processed to remove flat areas and the Planchon-Darboux method (Planchon and Darboux, 2002) was used to fill any remaining hollows.

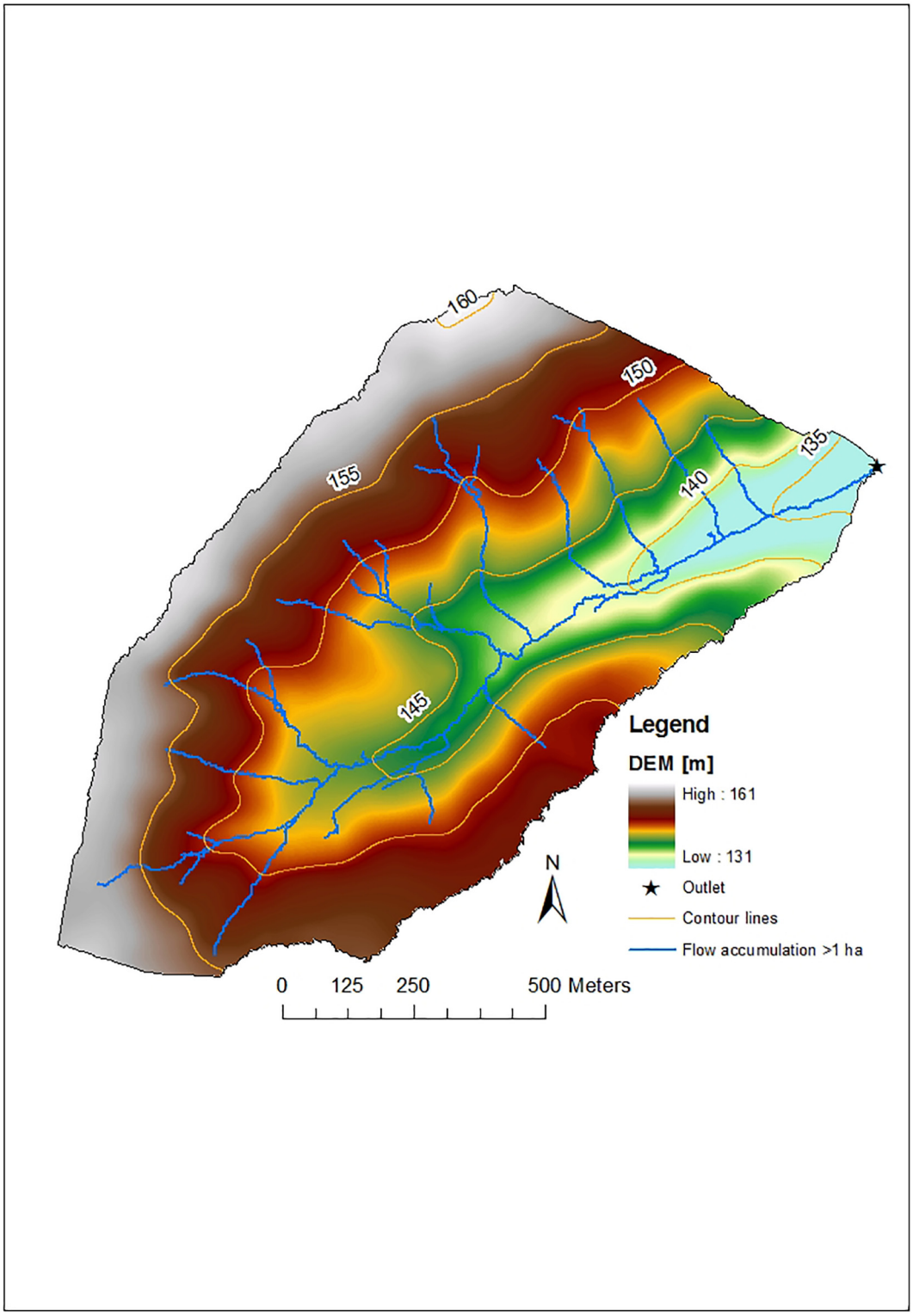

Fig. 1. Catchment DEM with flow accumulation.

Table 2
Overview of the scenarios of different fields and grass strips and grassed waterway (see Fig. 2). Note that the rainfall with a 1-yr return period was used only in the baseline scenario.

Scenarios	Rainfall	Abbreviations	Different crop allocation patterns	Number of simulations
Baseline	1 yr, 10 yr, 50 yr	BA_1, BA_{10}, BA_{50}	0	3
Small fields	10 yr, 50 yr	SF_{10}, SF_{50}	5	10
Medium fields	10 yr, 50 yr	MF_{10}, MF_{50}	5	10
Medium fields, conservation	10 yr, 50 yr	MF-$cons_{10}$, MF-$cons_{50}$	5	10
Large fields	10 yr, 50 yr	LF_{10}, LF_{50}	5	10
Medium fields with grass strips	10 yr, 50 yr	MF-$gras_{10}$, MF-$gras_{50}$	5	10
				Total: 53

For the purpose of the modelling exercise, the catchment characteristics were simplified in order to restrict the number of factors that could interact with the connectivity features being studied.

2.3.2. Scenario description

A total of 53 scenarios were simulated with each model in which field size and orientation was varied, and soil conservation measures (grass strips, grassed waterway) were implemented. An overview of the scenarios is given in Table 2. All models were first implemented using a baseline scenario assuming a bare soil and no field borders across the entire catchment. Three 1-hour block rainfall events of 1, 10 and 50 year return periods were simulated. Rainfall intensity was selected based on intensity-duration-frequency curves for Chastre (Belgium) for these return periods (Table 3). Constant rainfall was assumed as it facilitates interpretation of the hydro- and sedigraphs. As the 1-year return period event did not produce any runoff in the baseline scenario, in subsequent scenarios only rainfall events with 10 and 50-year return periods were evaluated in subsequent scenarios.

Table 3
Rainfall duration and intensity as used by all models for the 1, 10 and 50-year return periods.

Rainfall	Unit			
Return period	year	1	10	50
Duration	minute	60	60	60
Constant intensity	$mm \cdot h^{-1}$	17.4	29.9	38.7
Kinetic energy	$MJ \cdot mm^{-1} \cdot ha^{-1}$	0.203	0.243	0.260

The catchment was divided into fields of roughly equal size. The size and orientation of the fields varied among scenarios. Three field sizes were evaluated: large (average of 20.7 ha each), medium (10.3 ha) and small (5.2 ha). In the standard scenarios (non-conservation), the fields in the north-eastern half of the catchment were typically oriented along the slope (Fig. 2a, b, c). The fields converge towards an axis that runs from the catchment head to the catchment outlet and which coincides or runs close to the main drainage axis of the catchment. This is similar to the real catchment on which the semi-virtual catchment is based. For the medium-sized fields, an additional scenario was considered, in which the fields in the north-eastern half of the catchment were oriented perpendicular to the slope (Fig. 2d). This scenario is referred to as 'conservation'. A fifth scenario was designed in which the standard medium-size plots were combined with grass strips and a grassed waterway (Fig. 2e). The grass strips and grassed waterway occupied 2% of the total area of the catchment. The grassed waterway was located along the main drainage axis of the catchment, towards its downstream end. The grass strips were located perpendicular to the slope to reduce the length of the longest fields. Some strips were also located to intercept the flow axis. Characteristics of the grass strips and grassed waterway are provided in Table 5. Tillage was assumed to

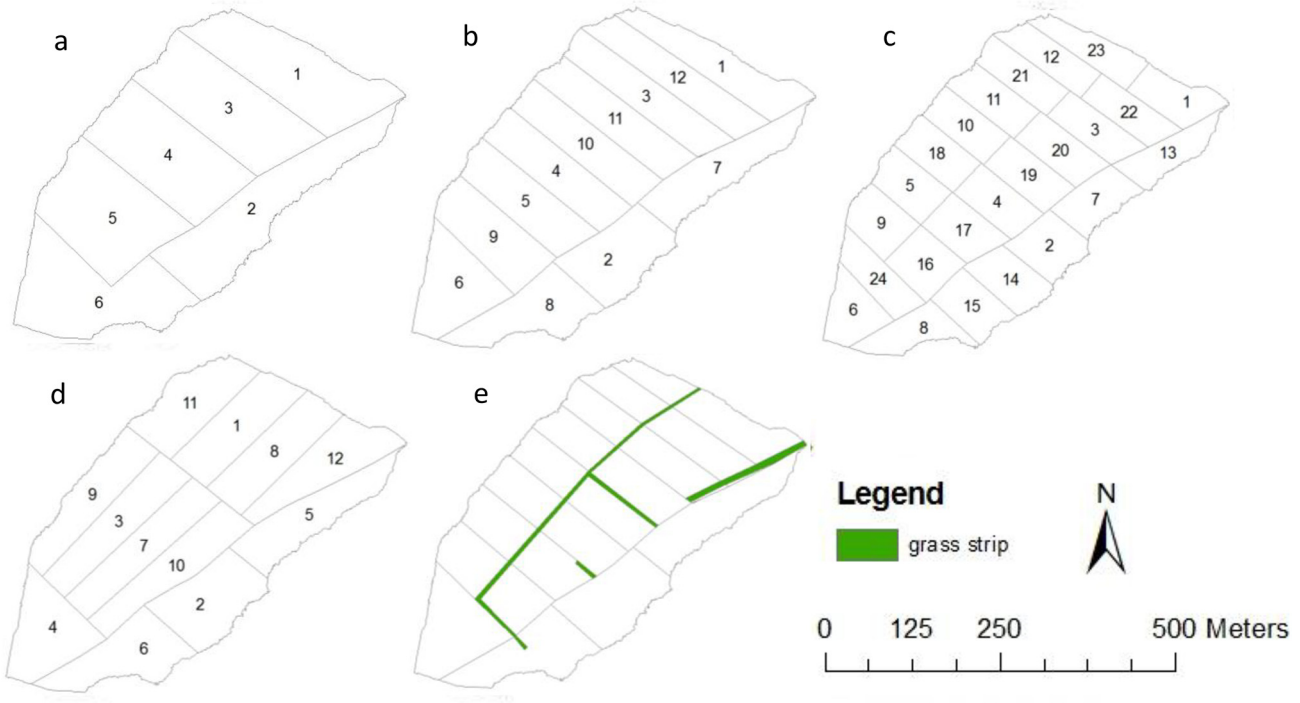

Fig. 2. The various scenarios of field size and orientation with (a) large fields, (b) medium-sized fields, (c) small fields, (d) medium-sized fields oriented perpendicular to the slope ('conservation') and (e) medium sized fields with grass strips and grassed waterway (depicted in green). (For interpretation of the references to colour in this figure legend, the reader is referred to the online version of this chapter.)

occur parallel to the main slope for all scenarios except for the conservation scenario where it is perpendicular to the slope.

A total of five land use patterns were considered for each field size and/or field orientation (Table 4). To facilitate model comparisons, only two crops were considered: winter wheat and sugar beet. In the Belgian loess belt, it is common to have rotations in which spring crops and winter cereals alternate. The main winter cereal is winter wheat. Sugar beet and potatoes are the two main spring crops. Because potatoes are cultivated on ridges which have a strong impact on within-plot flow connectivity, sugar beet was selected.

2.3.3. Input data

Besides the DEM, the models need input data on soil, surface and vegetation characteristics. A single homogeneous soil type was imposed, whose characteristics are typical of the dominant soils found in the region (Table 4). The virtual silt loam soil is deep, free of stones and vertically homogeneous.

Crop type has an impact on surface roughness, crusting, and soil cover by vegetation, and these factors evolve over time. For the purpose of this modelling exercise, the vegetation characteristics were defined so as to correspond to the month of May (Table 5). This month is a critical period regarding erosion and muddy floods because of the still low vegetation cover of spring crops, extensive surface sealing and the frequent occurrence of high erosivity thunderstorms (Evrard et al., 2007). For each field size and orientation scenario (Table 2), five different crop allocation patterns were considered while maintaining the proportion of sugar beet and winter wheat constant (about 50% each). Details of the crop allocation patterns can be found in the supplementary material.

Table 4
Soil parameters for all scenarios (adapted from Laloy (2010) and Laloy and Bielders (2008)).

Soil property	Unit	Value
Vol. water content initial (field capacity)	$m^3 \cdot m^{-3}$	0.38
Vol. water content wilting point	$m^3 \cdot m^{-3}$	0.16
Vol. water content saturated	$m^3 \cdot m^{-3}$	0.49
Particle density	$kg \cdot m^{-3}$	2650
Bulk density	$kg \cdot m^{-3}$	1350
Stoniness	%mass	0
Depth	m	2
Sand (50–2000 μm)	%	14
Silt (2–50 μm)	%	69
Clay (<2 μm)	%	17
Soil organic carbon content	$g \cdot kg^{-1}$	11
Matric head at wetting front (Green & Ampt)	mm	250
Median diameter (d50)	μm	35
Soil cohesion	kPa	7
Aggregate stability according to drop test	No. of drops	10

2.4. Analysis of model results

Model results were stored in two maps per scenario, containing total transfer of water (m^3) and sediment (kg) through a cell, respectively, at the end of each simulation. These maps were subsequently analysed using an automated approach programmed in Python (version 3.5).

The following variables related to functional connectivity were analysed and compared: (1) total export of water (m^3) or sediment (kg) per cell, (2) active water or sediment area (m^2; see below for explanation), (3) area connected to the catchment outlet (m^2) defined as the area of water or sediment active cells for which there is a continuous path of active cells until the outlet.

Models were not calibrated. However, as indicated earlier, a prerequisite of inclusion for the models was that they had already been evaluated successfully against data in similar conditions as the semi-virtual catchment used in the present study. Watersed and LandSoil are derived from Stream, which was applied by Evrard et al., 2009 in Central Belgium. OpenLISEM was originally developed in the Loess area of South Limburg (NL; De Roo et al., 1996a, 1996b. FullSWOF_2D is a generic Shallow Water equations solver, previously used from agricultural plots (Peñuela et al., 2016) to urban catchments (Hong et al., 2016). The main reason not to calibrate the models was that it might erroneously rank models according to accuracy, which would distract from the purpose of the current study (i.e. to compare model output in terms of connectivity). However, calibration was replaced by a model assessment to ensure that all provide results in a similar range for the baseline scenario, such as producing runoff and sediment yield within credible bounds. To allow a reasonable comparison between the models, all model scenario results were also normalized against the baseline results of each model. Water and sediment exports from all scenarios were therefore expressed as exports relative to the baseline scenario for the specific return period.

Determining whether a cell is active or not requires defining a threshold value for water or sediment transfer below which the cell is considered inactive. The normalization for the comparison of area connected to the outlet was done based on defining the catchment to be

Table 5
Surface and vegetation characteristics specific for each land use type.

Parameters	Unit	Bare	Wheat	Sugar beet	Grass strip
Crusting stage[a,b]	–	F2 (sedimentary stage)	F12 (local depositional crusts)	F12	F0 (fragmentary stage)
Roughness index[a,b]	–	R0 (0–1 cm)	R1 (1–2 cm)	R1 (1–2 cm)	R1 (1-2 cm)
Cover index[a,b]	–	C1 (0–20%)	C3 (61–100%)	C1 (0–20%)	C3 (61–100%)
Final infiltration capacity – Saturated hydraulic conductivity[c]	$mm \cdot h^{-1}$	10	50	20	20
Sediment concentration – interrill[c]	$g \cdot l^{-1}$	3	5	10	0
Manning's n[d]	SI units	0.010	0.024	0.015	0.30
Random roughness (RR)[e]	mm	6	6	6	12
Depression storage	mm	$=10^*((0.327–0.037^*slope+0{,}0012^*slope^2)$ $^*RR+(-0.017+0.007^*slope-0.0002^*slope^2)^*RR^2)$			
Oriented roughness height	mm	0	20	20	12
Vegetation cover[e]	%	0	70	10	100
Vegetation height[e]	cm	0	35	7.5	15
Residue cover	%	0	0	0	0

[a] Based on the typology used in the STREAM model (Cerdan et al., 2002b).
[b] Based on Evrard et al. (2007).
[c] Based on Evrard et al. (2009).
[d] Based on Maugnard (2015).
[e] Based on GISER (2011).

75% active during the 10 year return period storm with baseline settings. The thresholds for determining whether a cell is active or not for each model was then determined by calculating the 75th percentile in the export values for water.

Model results were compared on four different factors to explain the simulation results in terms of relative exports and connected areas: rainfall (10 and 50-yr return period), field size (small, medium, large), crop allocation pattern (different spatial patterns of sugar beet and winter wheat; see supplemental material) and conservation measures (field orientation and/or grass strips and grassed waterways for medium-sized fields). In order to rank the relative importance of these factors, the following calculation was performed: the relative export and the connected area at the outlet were calculated for all the runs. Then, for each of the four factors separately, these results were grouped into classes (e.g. the 10 year return period results were separated from the 50 year return period). The mean of each class was then calculated and the absolute value of the difference between the highest and the lowest mean was determined. This difference, hereafter referred to as the Absolute Mean Difference (AMD), therefore reflects the range of mean values across the different classes for a given factor, and thus the extent to which the considered factor influences models results. These calculations were repeated for each model separately.

Finally, models and scenarios were compared in terms of structural connectivity. The structural connectivity of the various scenarios was assessed using the Index of Connectivity (IC; Borselli et al., 2008; Cavalli et al., 2013), calculated using the SedInConnect tool (Crema and Cavalli, 2018). The USLE C-factor was used as weighing factor with values of 0.44 for sugar beet, 0.36 for winter wheat and 0.003 for grass strips. These C-factor values were calculated according to Maugnard et al. (2013). The 99th percentile of each IC map was taken as an indicator for spatial connectivity (de Walque et al., 2017) and the scenarios were ranked in order of decreasing connectivity. Model simulation results were compared in terms of connectivity in two different ways: (1) how much the models agree or disagree regarding the connected area of both runoff and sediment, averaged over all scenarios and (2) the correlation between pairs of models on different scenarios, indicating if models react similarly to different scenarios or not.

3. Results

3.1. General behaviour of models

The Absolute Mean Difference (AMD) calculations revealed important patterns in the behaviour of the models (Table 6). For the different scenarios, rainfall is the main factor affecting the relative exports as well as the connected area, for both water and sediment in all models except for FullSWOF-2D which produced no runoff for any of the scenarios except the baseline. The land use and conservation measures had smaller and varying influence on the water and sediment exports and connectivity. For OpenLISEM, crop allocation pattern ranks second in the AMD, while for Erosion 3D conservation practices rank second. For LandSoil and WaterSed, field size is the second most important factor. Except for Erosion 3D, conservation practices had the smallest influence on the simulated water and sediment exports and connected areas (Table 6).

It is also interesting to note that the rankings of water relative export and water connected area were closely related for all models, whatever the considered factor (e.g. field size, crop allocation or conservation measure). Consequently, the variations in relative water exports were mostly induced by variations in the connected area. In other words, water export decreased or increased when the land use variations implied a disconnection or a connection of a part of the catchment. This situation can be explained by the relatively simple geometry and configuration of the catchment, with a single main channel draining the whole catchment area.

In case of sediment export and connected area, a similar ranking between both parameters was only found for OpenLISEM. It implies that the spatial variations of the land use had important impacts on the simulated sediment transfer for most of the models.

3.2. Rainfall effects on simulated relative exports and connected area

The increase in rainfall depth when modelling 10-yr and 50-yr return periods had the most substantial effect on the relative water and sediment export and the connected area in almost all scenarios (Fig. 3). For almost all models, the connected area increases as the rainfall return period increases.

The different land-use scenarios had in general higher infiltration rates (factor 2 to 5) and Manning's n values (factor 1.5 to 2.4) than the baseline scenarios. The export of water and sediment are therefore <50% of the baseline scenarios and the connected areas are <60% of the baseline for all models, except FullSWOF_2D which did not produce surface runoff for any of the scenarios except the baseline (Fig. 3).

The rainfall return period affected the relative sediment export more than the relative water export. The median relative water exports were 0% (FullSWOF_2D), 4% and 20% (Watersed), 7% and 21% (OpenLISEM), 9% and 20% (Erosion3d), and 18% and 27% (LandSoil), respectively for the 10-year and 50-year return period. The respective median relative sediment exports were 4% and 14% (Watersed), 4% and 13% (OpenLISEM), 9% and 20% (Erosion3d), and 20% and 31% (LandSoil). Thus, rainfall is an important factor controlling water and sediment relative exports, whatever the considered model structure.

The higher scatter in the connected area values for the different land use scenarios for LandSoil and, to a lesser extent, for Erosion3D, implied that the differences in connected area induced by the change in rainfall return period was less important relative to land use variations for these

Table 6
Ranking of the Absolute Mean Difference (AMD; values between brackets) in Water Relative Export (WRE), Sediment Relative Export (SRE), Connected Area Water (CAW), and Connected Area Sediment (CAS) as affected by the factors rainfall, field size, crop allocation pattern and conservation measures. Ranks from 1 (highest) to 4 (lowest) also illustrated by colour coding from dark to light colour.

Model	Erosion 3D				OpenLisem			
	WRE	SRE	CAW	CAS	WRE	SRE	CAW	CAS
Rainfall	1 (0.119)	1 (0.088)	1 (0.320)	1 (0.320)	1 (0.140)	1 (0.095)	1 (0.337)	1 (0.267)
Field size	4 (0.034)	4 (0.036)	4 (0.041)	4 (0.035)	3 (0.009)	4 (0.017)	3 (0.003)	4 (0.007)
Crop allocation	3 (0.046)	2 (0.086)	3 (0.047)	3 (0.048)	2 (0.025)	2 (0.037)	2 (0.027)	2 (0.056)
Conservation	2 (0.087)	3 (0.040)	2 (0.053)	2 (0.057)	4 (0.007)	3 (0.020)	4 (0.001)	3 (0.010)

Model	Landsoil				WaterSed			
	WRE	SRE	CAW	CAS	WRE	SRE	CAW	CAS
Rainfall	1 (0.094)	2 (0.112)	1 (0.132)	1 (0.131)	1 (0.160)	1 (0.110)	1 (0.290)	1 (0.290)
Field size	2 (0.044)	1 (0.149)	2 (0.063)	2 (0.064)	2 (0.017)	2 (0.010)	3 (0.003)	3 (0.003)
Crop allocation	3 (0.017)	3 (0.053)	3 (0.055)	3 (0.054)	3 (0.010)	4 (0.004)	2 (0.008)	2 (0.008)
Conservation	4 (0.006)	4 (0.032)	4 (0.039)	4 (0.042)	4 (0.005)	3 (0.007)	4 (0.001)	4 (0.002)

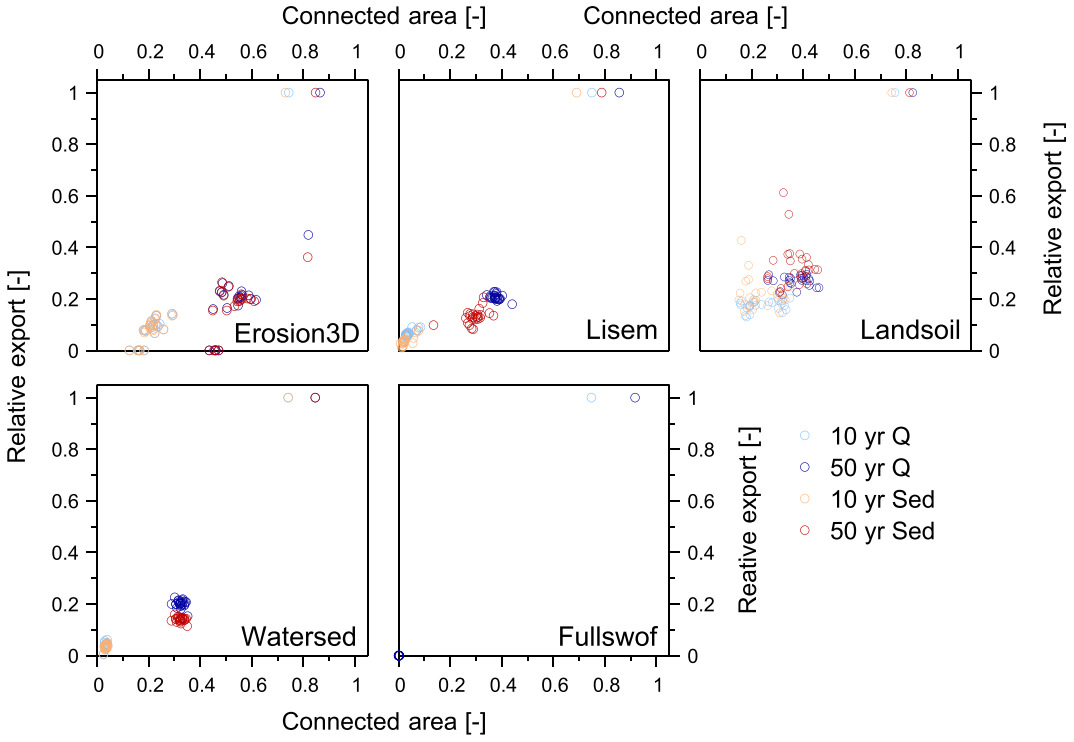

Fig. 3. Relationships between relative exports and connected area for the 53 scenarios and each of the five models. Red dots represent relative sediments exports (Sed in legend) while blue dots represent relative water exports (Q in legend). Lighter coloured dots represent the 10-year rainfall return period, darker coloured dots the 50-year return period. The four dots with a value of 1.0 for relative export represent the simulated results for the reference baseline scenarios. (For interpretation of the references to colour in this figure legend, the reader is referred to the online version of this chapter.)

models. Indeed, the connected area of the two return periods overlapped, for instance for the relative water export with minimum and maximum values of 0.16 and 0.35 for the 10-year return period, and 0.26 and 0.46 for the 50-year return period. Watersed and OpenLISEM simulated relatively constant connected area. The connected area for LandSoil is similar for the water and the sediment export, although the relative sediment export is higher than the relative water export. This result is likely to reflect the increased interrill sediment concentrations in the different land-use scenarios relative to the baseline scenarios, because of less pronounced crust development. Conversely, Erosion3D and Watersed showed very similar behaviour between the relative sediment and water export, indicating that the higher crop cover compensated the increase in sediment interrill erosion. Indeed, higher crop cover implied both higher Manning's *n*, smaller interrill concentration and smaller probability of concentrated erosion.

3.3. Land use and conservation practices effects on simulated exports

Comparing model results for the different models and scenarios first of all indicates that differences in relative water and sediment export between different models are often larger than between different scenarios (Fig. 4). Beside the general difference in model outputs there is no overall agreement between models regarding the effects of field sizes, some models simulating higher relative water and sediment export on large fields (e.g. LandSoil, Watersed), while others simulated higher relative water and sediment export on small fields (e.g. OpenLISEM). However, all models simulated a high variability between the different scenarios with mid-sized fields (i.e. medium fields conventional vs. medium fields with conservation and medium fields with grass strips). In addition, more variation was generally simulated for relative export of sediment as compared to relative export of runoff, except for Watersed, where the variation between crop allocations is small for both relative runoff and sediment. Both LandSoil and OpenLISEM show relatively lower relative sediment export for medium-sized fields with grass strips, even though the relative runoff for this scenario was not lower compared to the other scenarios. Erosion3D shows low runoff and sediment export for the conservation scenario, while LandSoil shows a wider range in relative sediment export for the conservation scenario as compared to the other scenarios.

From the AMD results, it can be seen that the conservation practices scenarios had limited influence on the models results (Table 6). The conservation practices scenarios represented on average (over the different models) 97% of the median water relative export (Fig. 4). Consequently, this factor ranked fourth for most of the models and variables. The exception was Erosion3D (Table 6, Fig. 4), ranking conservation practices second. Indeed, for this model, the conservation practices scenarios represented 15% to 12% (respectively for the 10-yr and 50-yr return period) of the median relative export of the non-conservation scenario modelled with the same field layout. The grass strips had lower infiltration capacity relative to that of the wheat crops, respectively 20 mm h^{-1} and 50 mm h^{-1}, nonetheless the effect of this decrease in infiltration capacity of the grass strip remains low in comparison to the excess runoff water induced by the two rainfall events. Indeed the rainfall amount difference affects the entire catchment area, whereas the grass strip only impact a very limited area (2%). Consequently, the models simulated slightly higher (mean across all models: 108%) relative runoff in the scenario including grass strips compared to the conventional medium-sized fields. However, the high Manning's *n* (0.3) and random roughness (12 mm) of grass strips resulted in lower simulated sediment export (mean across all models: 80%).

Field size was an important factor for LandSoil and Watersed, but ranked lowest for OpenLISEM and Erosion3D. This can be explained by the important variations in the field characteristics induced by changes in crop allocation (for instance, infiltration capacity dropped from 50 mm h^{-1} for wheat to 20 mm h^{-1} for sugar beet, see Table 5 for details). Runoff was therefore easily infiltrated/generated when flowing across

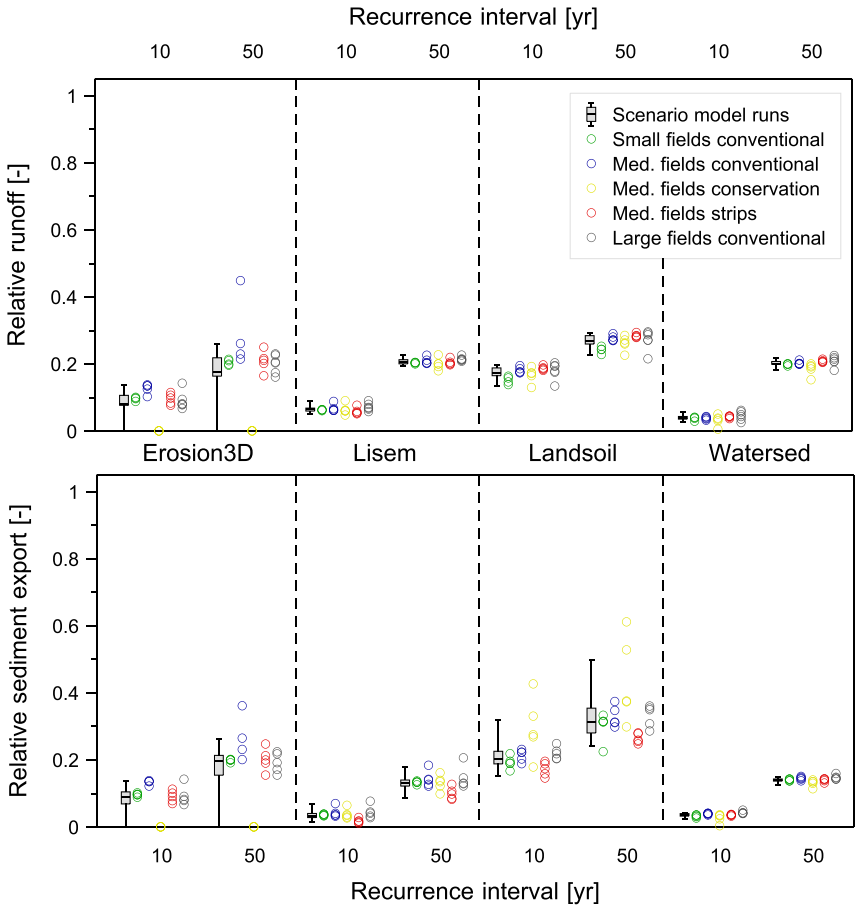

Fig. 4. Modelled relative water (upper graphs) and sediment (lower graphs) export differentiated for the five field designs (see Fig. 2); boxplots summarise the scenarios and field designs for each recurrence interval and model. Boxplots give median, 1st and 3rd quartile and 5% and 95% quantiles. Note: FullSWOF_2D is not included as it does not produce runoff for the scenarios.

the different crop allocations, with limited influence on the runoff length.

3.4. Model comparison regarding structural connectivity

Boxplots of the IC value distributions are shown in Fig. 5, clearly showing that the mean of the grass-strip scenarios is lower than the other scenarios. The 99th percentile of the IC connectivity index for all scenarios varied between −3.46 and −4.00. Ranking this for the different scenarios from high to low connectivity (Table 7), again clearly shows that the scenario with conservation strips always results in lowest IC values. Other scenarios do not rank in terms of connectivity in a clear order; for example, a scenario with large fields does not necessarily always result in higher connectivity. However, on average, scenarios with large fields result in higher connectivity and medium fields with conservation orientation (i.e. perpendicular to the slope, see Fig. 2d) result in the lowest average connectivity (except for the grass strips scenarios). The land use pattern also affects the connectivity ranking, with an important role of the field closest to the outlet: for the land use pattern 3, 1 and 4 for large fields the field closest to the outlet (field 1 – Fig. 2a) is cultivated with sugar beet, which has a relatively low infiltration rate compared to winter wheat (Table 5). This is also the case for the small field configuration with land use patterns 3 and 2, the conventional medium fields with land use pattern 1 and 4 and for the medium conservation field with land use pattern 1 and 4. These combinations of field size/orientation and crop allocation pattern result in the highest 99th percentile IC values (ranks 1–9).

We also tested how much the models agree (or disagree) regarding the connected area of runoff and sediment (Fig. 6). Fig. 6 a and b show the total area of agreement between pairs of models, averaged over all scenarios, for runoff (Fig. 6a) and sediment (Fig. 6b). The upper right part of the figure shows the results of the 10 yr return period event while the lower left part of the figure shows the results for the 50 yr return period event. Fig. 6c and d show the agreement of the connected area only, for runoff (Fig. 6c) and sediment (Fig. 6d). Thus, total area of agreement sums up cells with the same outcome (connected or not connected) for a pair of models. The matrix of agreement on connected areas (Fig. 6c and d) only sums up cells of agreement on connected areas. Hence, models that show very low connectivity have a high total area of agreement (many cells in both models will be 'not connected') but may have a small area of agreement on connected areas (if the few cells that are 'connected' in each model, are not the same cells). Area of agreement on connected runoff and sediment is much lower than total area of agreement, and it is higher for the 50-yr return period than for the 10 yr return period. Area of agreement on the connected area is highest for the LandSoil- Erosion 3D combination for sediment and for the combinations LandSoil-Erosion 3D, OpenLISEM-Erosion3D and OpenLISEM-Watersed for runoff. Total area of agreement is higher for the 10 yr as compared to the 50 yr return period event, while the opposite trend can be seen for the agreement of the connected area, indicating that for the 10 yr event many cells were unconnected, due to limited runoff production in this event.

Fig. 6e and f show the correlation on total connected area between model pairs on different scenarios. Hence, these values indicate if the models react similarly on different scenarios or not. As FullSWOF_2D did not produce runoff for the 10-yr recurrence rainfall, the correlation

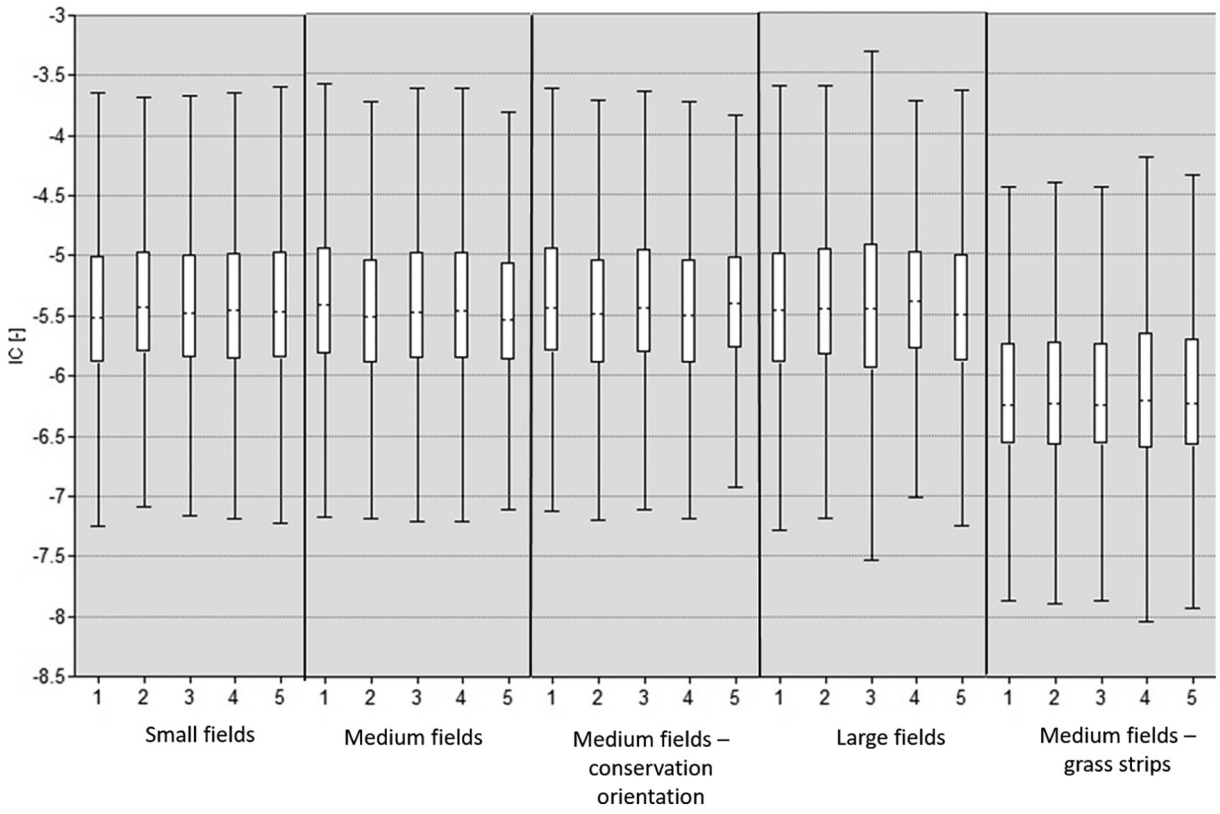

Fig. 5. Boxplots of IC values for the 25 scenarios. 1–5 refers to the crop allocation pattern (see supplementary material).

was not calculated for these scenarios. Correlation between models is generally low, with highest correlation between the combination Erosion3D - Watersed for the 10-yr event for both runoff and sediment (but not for the 50 yr-return period), and between Erosion3D and LandSoil for both runoff and sediment, and both 10-yr and 50-yr events. There is also good correlation between Watersed and OpenLISEM for the 50-yr return period for both runoff and sediment.

Fig. 6g and h show the average connected area of a model for all scenarios for runoff (Fig. 6g) and sediment (Fig. 6h). The average connected area is, as might be expected, higher for the 50-yr return period event as compared to the 10-yr return period event. For the 10-yr return period event, Erosion 3D and LandSoil show relatively high values for the connected area for both runoff and sediment, while for the 50 yr return period event, Erosion 3D shows higher values and LandSoil, OpenLISEM and Watersed are in the same range.

Table 7
99th percentile of IC values, ranked for all scenarios. Grey: large fields conventional, blue: medium fields conventional, green: small fields conventional, yellow: medium fields conservation, orange: medium fields grass strips.

	Scenario		
Rank	Field map	Crop allocation pattern	99th percentile IC [-]
1	Large fields	3	-3.46
2	Medium fields; conservation	1	-3.49
3	Medium fields; conservation	4	-3.53
4	Small fields	3	-3.55
5	Small fields	2	-3.56
6	Medium fields	1	-3.56
7	Large fields	1	-3.58
8	Large fields	4	-3.58
9	Medium fields	4	-3.59
10	Large fields	5	-3.62
11	Small fields	1	-3.62
12	Small fields	5	-3.62
13	Medium fields	3	-3.63
14	Medium fields	2	-3.64
15	Small fields	4	-3.64
16	Large fields	2	-3.66
17	Medium fields; conservation	5	-3.66
18	Medium fields	5	-3.67
19	Medium fields; conservation	3	-3.67
20	Medium fields; conservation	2	-3.75
21	Medium fields with grass strips	1	-3.95
22	Medium fields with grass strips	2	-3.97
23	Medium fields with grass strips	3	-3.96
24	Medium fields with grass strips	4	-3.93
25	Medium fields with grass strips	5	-4

4. Discussion

4.1. Model results and comparison

From the factors that were tested, difference in rainfall amount (here 29.9 mm h^{-1} versus 38.7 mm h^{-1}, each event lasting 1 h; see Table 3) plays the most important role in the simulated differences between models, in terms of relative export and connected area of runoff water and sediment (Table 6, Fig. 3). All models therefore indicated that changes in the amount of rainfall influenced connectivity more than landscape elements, at least in case of our pronounced differences in recurrence intervals (10 yr and 50 yr). This finding, however, depends on the scenario choices – if we had considered a narrower range of rainfall events and a wider range of field sizes or conservation scenarios, the findings might have been different. The present result implies that functional aspects of connectivity were more important than structural connectivity itself (sensu Bracken et al., 2015, 2013). This result is consistent with the observation that in case of very high intensity storms large erosion and sediment delivery occur even under soil conservation measures (e.g. Fiener et al., 2019). On the other hand, several studies report the importance of (changes in) landscape structure for

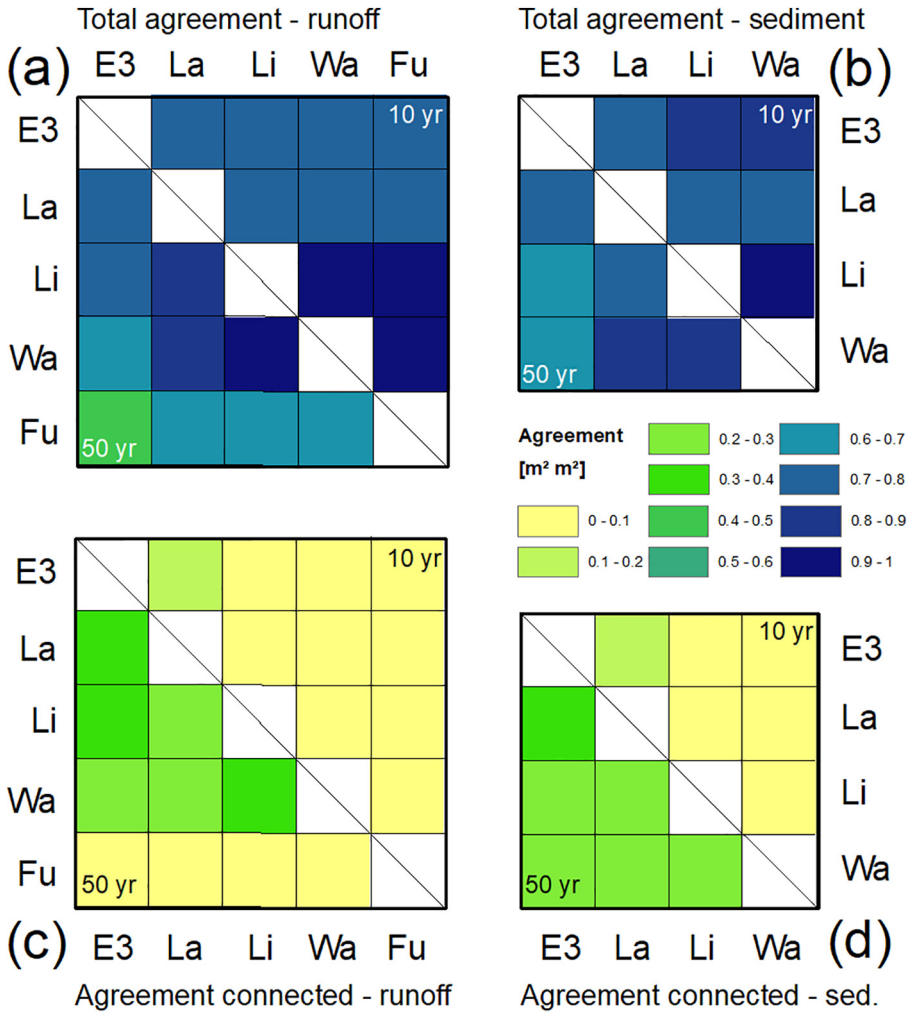

Scenario correlation - runoff

(e)

50 yr recurrence \ 10 yr recurrence	E3	La	Li	Wa	Fu
E3	-	0.31	0.08	0.44	-
La	0.12	-	0.00	0.12	-
Li	0.01	0.01	-	0.03	-
Wa	0.00	0.00	0.43	-	-
Fu	0.03	0.02	0.06	0.16	-

Scenario correlation - sediment

(f)

50 yr recurrence \ 10 yr recurrence	E3	La	Li	Wa
E3	-	0.31	0.06	0.50
La	0.14	-	0.00	0.14
Li	0.01	0.02	-	0.01
Wa	0.00	0.00	0.14	-

(g) **Mean connected area all scenarios - runoff**

recur.	E3	La	Li	Wa	Fu
10 yr	0.21	0.24	0.04	0.03	0.00
50 yr	0.52	0.37	0.38	0.32	0.00

(h) **Mean connected area all scenarios - sediment**

recur.	E3	La	Li	Wa
10 yr	0.20	0.24	0.03	0.03
50 yr	0.52	0.37	0.29	0.32

Fig. 6. Model agreement regarding the total area (connected and unconnected) for runoff (a) and sediment (b); model agreement for the connected area only for runoff (c) and sediment (d). Colours indicate the mean area of agreement averaged over all scenarios; (e) and (f) show the correlation on total connected area between model pairs on different scenarios for runoff (e) and sediment (f). (g) and (h) show the connected area, averaged over all scenarios, for runoff (g) and sediment (h). E3: Erosion3D, LA: LandSoil, Li: OpenLISEM, Wa: Watersed, Fu: FullSWOF_2D.

connectivity and catchment sediment dynamics. For example, Reulier et al. (2019) conclude that structural elements (hedgerows, water ways and cultivated land use versus grassland) affect catchment connectivity in a lowland agricultural catchment. Cossart and Fressard (2017) also show the importance of landscape structure for sediment dynamics in a mountainous catchment. Both studies did not include functional connectivity though. Cossart et al. (2018) presented a case study in which they study process-based (functional) connectivity using differential modelling, revealing a self-organised catchment response that was not always directly coupled to meteorological forcing. However, their study catchment was more complex than the semi-virtual catchment used in this study and the main cause for the lack of relation between rainfall and catchment response was sediment exhaustion, which does not play a role in our study. Finally, David et al.

(2014) analysed catchment hydrological and sediment response for various scenarios of land use change and landscape design. They concluded that land use choices are more important in sediment response than landscape design (e.g. grass strips, waterways, roads etc.).

As for the role of structural landscape elements, there was no overall agreement between models regarding the effects of field sizes, crop allocation pattern and conservation practices (Table 6, Fig. 4). Conservation measures influenced the relative export and connected area mainly for Erosion3D, but much less for the other models. Crop allocation pattern was more important for OpenLISEM and LandSoil (Table 6), which is in line with findings by David et al. (2014). As shown in Fig. 4, the models did not agree on the impact of field size, field orientation and grass strips. As an extreme example of this, both models that include tillage direction (Erosion3D and LandSoil) agree that the conservation field configuration has a large effect, but in one case it increases erosion (LandSoil) and in the other sediment export is decreased (Erosion3D). This example shows that the parameterization and way in which tillage direction is implemented in the model affects model results. Similar disagreement between models can be observed when comparing the connectivity index (IC) with model results for grass strip scenarios: while the calculated IC values are clearly lowest for grass strips (Table 7), not all models simulate the lowest sediment export in grass strip scenarios (Fig. 4).

Furthermore, in most scenarios except grass strips, the crop assigned to the outlet appears to be important for structural connectivity (as calculated using the 99th percentile of IC). A similar finding was reported by David et al. (2014) who related a higher sediment delivery to inappropriate land use types and spatial allocations (in their case orchard located near the watershed outlet without linear landscape features between the eroding orchard field and the stream network). However, this result is somewhat biased by ranking the scenarios using the 99th percentile of IC: the highest IC values appear at the outlet when the crop is sugar beet, which has a higher C-factor than winter wheat. When ranking the scenarios on e.g. median IC values, the ranking changes and the importance of the crop at the outlet disappears.

There was also low agreement between models on the spatial patterns of connectivity. Total area of agreement was high only for the high rainfall scenario, but even in this case the agreement on the location of the connected areas was low. One possible explanation would be that differences in runoff and sediment simulation in individual cells are compounded by differences in flow and sediment routing simulations, meaning that spatial errors accumulate. However, previous erosion model comparisons with field data (Jetten et al., 2003; Nunes et al., 2005) have shown that while models tend to agree with field-averaged data, the simulation of small-scale patterns is usually not good. The authors attribute this to the parameterization of soil and vegetation processes at the field scale rather than the individual cell scale. For this exercise, this means that the small-scale differences between models are unavoidable and probably also different from observed patterns. However, recent developments in integrating satellite imagery and spatially-distributed soil data (e.g. Tavares Wahren et al., 2016; Van Eck et al., 2016) might help alleviate this problem in the future.

The overall disagreement between models was unexpected. Although differences were expected, we did expect models to agree more in general, for example by showing a general trend (for all models) of decreasing sediment export going from larger to smaller fields and from orientation along the slope to orientation perpendicular to the slope. However, such trends were not observed for the used models. Because we selected models in this study that include the relevant processes in the study catchment, that have been shown to perform adequately under similar conditions, are spatially distributed and that run on an event basis, the models included in this study are similar. However, there are still, obviously, differences between the models (see Section 2.2 and Table 1). The difference in 'fine' structure could be solved by calibration (i.e. parameterization is important). However, underlying individual equations (i.e. model structure) also play role in the different outcomes, as shown for example by the findings that the 'dynamic' models (i.e. those with multiple timesteps within the event, see Table 1) do not agree.

Unfortunately, there is a lack of studies comparing models across different field and crop configurations and erosion control measures to compare with the results of our study. However, previous model comparison exercises, although smaller in scope, did provide some indications as to the sources of this disagreement which concur with our results. When calibrated, erosion models tend to have similar performance for sediment yield predictions (Jetten et al., 2003, 1999; Shen et al., 2009). However, their simulation of connectivity is often different, as shown by different and sometimes quite contrasting predictions of hillslope erosion patterns despite similar parameterization and spatial data (Abdelwahab et al., 2018; Karamesouti et al., 2016; Starkloff and Stolte, 2014).

Nearing et al. (2005) compared the response of several erosion models to changes in rainfall and cover in two catchments, finding different sensitivities to both parameters. They observed that the sensitivity of each model varied between study sites, implying that parameterization of vegetation cover and soils in each site was behind sensitivity. More recently, Tan et al. (2018) compared the performance of lumped erosion models across 454 catchments with different characteristics, finding that model performance after calibration varied with land cover type and with the ability of each model to parameterize vegetation cover drivers for erosion. Vieira et al. (2018) and Wade et al. (2012) found that different erosion models with different structures had, after being calibrated, the same sensitivity to changes in erosion control practices in roads and burnt areas, respectively. Conversely, Karamesouti et al. (2016) found different responses for uncalibrated spatially distributed models to changes in vegetation cover. The common result from these comparison exercises is that the most important parameter behind model response was the parameterization of runoff and erodibility of different land covers and structural elements, concurring with the results of this exercise. However, uncertainty in both spatially explicit input data as well as model evaluation data (e.g. spatial erosion rates) is high and data are difficult to obtain (Batista et al., 2019).

Our results also concur with those of Takken et al. (2005), who applied an earlier version of the OpenLISEM model to the loess belt with different parameters for flow resistance, different equations for flow resistance modelling, and different spatial routing approaches (topography vs. tillage direction). This led to different predictions of both erosion and sediment connectivity (both erosion patterns and sediment yield). The choice of flow routing method and parameters, both external to OpenLISEM, had the largest impacts on model results, while the choice of model equations had the smallest impacts.

4.2. Impacts of the model comparison exercise settings

As indicated above, some results from the model comparison exercise might have been determined by the exercise study case and model application approach. First, the selection of the semi-virtual catchment impacted the exercise on (1) the topography, which might not have much impact given the limited effect of structural connectivity, as discussed above; and (2) the scenarios, which were based on local issues (field configuration, conservation measures) and crops (typical of the Belgian loess belt). For example, Karamesouti et al. (2016) found large differences in spatial predictions by changing the spatial distribution of vegetation after fire in two models. However, the connectivity problems and solutions in the semi-virtual catchment are representative of larger issues at the scale of the Loess belt and similar agricultural areas, making the results of this exercise – the lack of capacity for models to simulate changes in structural connectivity elements – relevant for soil conservation planning.

Second, the decision not to calibrate models with measured values could have impacted the results, if the model representation of runoff

generation and soil erosion in each crop is indeed more important than structural landscape elements. However, this decision allowed each modeler to select how best to represent loess belt crops without being forced to calibrate the model with outlet measurements, which might have led to good results for the wrong reasons (as happened to Starkloff and Stolte, 2014). A recent, interesting discussion on model calibration and evaluation can be found in Batista et al. (2019) who conclude that models are not currently thoroughly tested, that models do not systematically exceed each other in their predictive accuracy and that evaluating spatially distributed models (as applied in our study), requires spatially distributed data. One possibility to improve model comparability without inducing errors due to excessive focus on outlet measurements might be to allow calibration on spatial runoff and erosion patterns, to ensure that each model represents connectivity as faithfully as possible by its model structure. However, not only is this data difficult to obtain, but care must also be taken not to compare the skill of each modeler in simulating these patterns instead of the capacity of the underlying model structure (since a comparison of models is also a comparison of modellers, as argued by Jetten et al. (1999)). Other possibilities include the previous calibration of field-scale model results using experimental plot data (Centeri et al., 2009; Kinnell, 2017), ensuring similar crop parameterizations without calibrating for spatial structure or connectivity; or using artificial surfaces for the model experiments, such as artificial plots (Favis-Mortlock et al., 2000; Nunes et al., 2006) or even catchments (Gerwin et al., 2009).

Thirdly, a smaller issue might be the resolution selected to represent the virtual catchment, since cell size can have different impacts on the simulations for different models (Cochrane and Flanagan, 2005; Hessel, 2005; Starkloff and Stolte, 2014; Zhang et al., 2008); if cells become too large or too small, different connectivity processes may come into play which the models are not designed to address (Nunes et al., 2018). Resolution and DEM pre-processing methods (as done in this exercise for the underlying 10-m topography data) can also impact mapped connectivity patterns (Cantreul et al., 2018). However, we believe that the 1-m resolution selected in this exercise is adequate for the structure of the participating models, because the landscape elements included in the virtual catchment are well represented with this resolution. Finally, this modelling exercise and its outcomes are based on simulation of individual events with different recurrence time. Simulation of a continuous series of events may yield different results, as connectivity may develop over time (e.g. in the form of gullies). However, it was beyond the scope of the present paper to include this.

4.3. Implications for modelling and representing connectivity

The large impact of rainfall characteristics on model outcomes implies that, whatever the considered model, connectivity should not be calculated based on landscape characteristics alone, but also, or perhaps mainly, based on rainfall forcing. This is especially important for individual heavy rainfall events with high erosion potential. Fig. 6 suggests that models have similar patterns of connectivity when there is more rainfall and hence more runoff/erosion (even though the agreement is still low). For lower rainfall, the agreement is very low. Given (as described above) that the large-intensity rainfall events represent most sediment yield, it can be argued that the model agreement on connectivity is more important for the most erosive events, and conversely that the lower agreement for smaller rainfall events is not so important. Perhaps this could also be linked to the fact that erosion model performance increases with event magnitude, as demonstrated by Nearing (2000, 1998). However, smaller events may be important for the transport of fine substances such as ash deposited after wildfires (Bodí et al., 2014) or transport of substances absorbed onto fine soil particles, e.g. soil carbon (Wilken et al., 2017) and pollutants (Bento et al., 2018). In this case, the lower agreement between models for less intense rainfall events might indicate their worse performance to simulate this transport of light and fine substances.

The higher agreement for larger rainfall events indicates that the models are better at simulating connectivity when large rainfall forcings are present, i.e. when functional connectivity dominates over the structural elements of connectivity. Nunes et al. (2018) describe how distributed hydrological and erosion models such as the ones used in this exercise might miss connectivity processes occurring at a resolution below the grid cell, such as microtopography; these are likely to be more important for smaller storms, and hence the authors' suggestion of integrating functions to simulate these processes may improve the simulation of connectivity for low rainfall events.

The model outcomes also have strong implications for all connectivity indices based solely on morphological parameters such as the IC index, which may not be well suited for connectivity assessments. In this case, other indices incorporating functional connectivity might be better suited, although catchment-scale indices of this type are less common than structural connectivity indices and more complex to calculate (Heckmann et al., 2018). In fact, there was no direct relation between the calculated IC for a particular scenario and its simulated sediment export by the models used in this exercise. However, the IC has been reported to not represent the connectivity in a satisfactory way in lowland areas with gentle slopes (Gay et al., 2016; Poeppl et al., 2019). Therefore, this conclusion might not be valid for catchments where structural connectivity may play a larger role, such as the Alpine catchments studied by Cavalli et al. (2013); or in catchments experiencing much larger vegetation cover and soil changes than the crop shifts used in the present exercise, such as the burnt and logged catchments described by Martínez-Murillo and López-Vicente (2018).

5. Conclusions and outlook

In this study, we evaluated the response in terms of connectivity of five models to landscape connectivity features and explained the differences based on differences in model structure. A total of 53 scenarios in which field size and orientation was varied and soil conservation measures were implemented, and with varying rainfall intensities, were simulated with each model. All models were event- and process-based, spatially explicit water and soil erosion models: EROSION3D, FullSWOF_2D, LandSoil, OpenLISEM and Watersed.

The results of this exercise suggest that both differences in model equations as well as parameterization of these processes (i.e. runoff and sediment production and routing patterns) may explain the observed differences between models. While parameterization can be achieved with traditional erosion monitoring experiments, the differences in model structure may be resolved incorporating connectivity functions based on routing. Past examples include soil moisture and saturation (Kalantari et al., 2019; Nunes et al., 2009) or tillage direction (Takken et al., 2005); the results of our study suggest that these approaches should be generalized to other models.

Our results also suggest that structural connectivity indices may not suffice to represent connectivity in this type of catchments (relatively simple and monotonous land cover), and functional connectivity indices should be applied. Heckmann et al. (2018) propose several such indices, some of which include some sort of dynamic modelling. The same considerations on the appropriate parameterization of vegetation, structural elements and routing apply for models and indices.

Finally, the results suggest several ways to build on this modelling exercise in the future. First, more care should be taken to ensure that the models have similar parameterizations for each land-use, although sediment yield calibration should be avoided to prevent constraints to the simulation of connectivity patterns. Secondly, continuous modelling over time is an interesting option to see how connectivity develops over medium- to long time scales. Thirdly, further study areas should be selected for a comparison, especially those with more important structural connectivity features such as mountain landscapes or with more important land-use changes. And finally, gathering and sharing within

the scientific community of more spatially distributed runoff/runon and sediment transport data is recommended.

Acknowledgements

This paper forms part of the activities of the EU-funded COST action "CONNECTEUR" (ES1306; http://connecteur.info). Working group 3 (on "modelling connectivity") thanks CONNECTEUR for funding multiple workshops in Aveiro, Durham, Wageningen, Augsburg, Louvain-la-Neuve and Nancy during which this paper has been developed. JPN acknowledges funding by a Portuguese Foundation for Science and Technology grant (IF/00586/2015). We would like to thank three anonymous reviewers for their constructive comments which helped us to improve this paper.

Declaration of competing interest

The authors declare that they have no known competing financial interests or personal relationships that could have appeared to influence the work reported in this paper.

Appendix A. Supplementary data

Supplementary data to this article can be found online at https://doi.org/10.1016/j.geomorph.2020.107300.

References

Abdelwahab, O.M.M., Ricci, G.F., De Girolamo, A.M., Gentile, F., 2018. Modelling soil erosion in a Mediterranean watershed: comparison between SWAT and AnnAGNPS models. Environ. Res. 166, 363–376. https://doi.org/10.1016/j.envres.2018.06.029.

Ali, G.A., Roy, A.G., 2010. Shopping for hydrologically representative connectivity metrics in a humid temperate forested catchment. Water Resour. Res., 46 https://doi.org/10.1029/2010WR009442.

Antoine, M., Javaux, M., Bielders, C.L., 2011. Integrating subgrid connectivity properties of the micro-topography in distributed runoff models, at the interrill scale. J. Hydrol. 403, 213–223. https://doi.org/10.1016/j.jhydrol.2011.03.027.

Appels, W.M., Bogaart, P.W., van der Zee, S.E.A.T.M., 2011. Influence of spatial variations of microtopography and infiltration on surface runoff and field scale hydrological connectivity. Adv. Water Resour. 34, 303–313. https://doi.org/10.1016/j.advwatres.2010.12.003.

Baartman, J.E.M., Jetten, V.G., Ritsema, C.J., de Vente, J., 2012. Exploring effects of rainfall intensity and duration on soil erosion at the catchment scale using openLISEM: Prado catchment, SE Spain. Hydrol. Process. 26, 1034–1049. https://doi.org/10.1002/hyp.8196.

Baartman, J.E.M., Masselink, R., Keesstra, S.D., Temme, A.J.A.M., 2013. Linking landscape morphological complexity and sediment connectivity. Earth Surf. Process. Landforms 38, 1457–1471. https://doi.org/10.1002/esp.3434.

Batista, P.V.G., Davies, J., Silva, M.L.N., Quinton, J.N., 2019. On the evaluation of soil erosion models: are we doing enough? Earth-Science Rev. 197, 102898. https://doi.org/10.1016/j.earscirev.2019.102898.

Bento, C.P.M., Commelin, M.C., Baartman, J.E.M., Yang, X., Peters, P., Mol, H.G.J., Ritsema, C.J., Geissen, V., 2018. Spatial glyphosate and AMPA redistribution on the soil surface driven by sediment transport processes – a flume experiment. Environ. Pollut. 234, 1011–1020. https://doi.org/10.1016/j.envpol.2017.12.003.

Bielders, C.L., Ramelot, C., Persoons, E., 2003. Farmer perception of runoff and erosion and extent of flooding in the silt-loam belt of the Belgian Walloon Region. Environ. Sci. Pol. 6, 85–93. https://doi.org/10.1016/S1462-9011(02)00117-X.

Boardman, J., Vandaele, K., Evans, R., Foster, I.D.L., 2019. Off-site impacts of soil erosion and runoff: why connectivity is more important than erosion rates. Soil Use Manag. 35, 245–256. https://doi.org/10.1111/sum.12496.

Bodí, M.B., Martin, D.A., Balfour, V.N., Santín, C., Doerr, S.H., Pereira, P., Cerdà, A., Mataix-Solera, J., 2014. Wildland fire ash: production, composition and eco-hydro-geomorphic effects. Earth-Science Rev. 130, 103–127. https://doi.org/10.1016/j.earscirev.2013.12.007.

Borselli, L., Cassi, P., Torri, D., 2008. Prolegomena to sediment and flow connectivity in the landscape: a GIS and field numerical assessment. CATENA 75, 268–277. https://doi.org/10.1016/j.catena.2008.07.006.

Botticelli, M., Guercio, R., Magini, R., Napoli, R., 2018. A physically-based approach for evaluating the hydraulic invariance in urban transformations. Int. J. Saf. Secur. Eng. 8, 536–546. https://doi.org/10.2495/SAFE-V8-N4-536-546.

Bout, B., Jetten, V.G., 2018. The validity of flow approximations when simulating catchment-integrated flash floods. J. Hydrol. 556, 674–688. https://doi.org/10.1016/j.jhydrol.2017.11.033.

Bracken, L.J., Croke, J., 2007. The concept of hydrological connectivity and its contribution to understanding runoff-dominated geomorphic systems. Hydrol. Process. 21, 1749–1763. https://doi.org/10.1002/hyp.6313.

Bracken, L.J., Wainwright, J., Ali, G.A., Tetzlaff, D., Smith, M.W., Reaney, S.M., Roy, A.G., 2013. Concepts of hydrological connectivity: Research approaches, pathways and future agendas. Earth-Science Rev. 119, 17–34. https://doi.org/10.1016/j.earscirev.2013.02.001.

Bracken, L.J., Turnbull, L., Wainwright, J., Bogaart, P., 2015. Sediment connectivity: a framework for understanding sediment transfer at multiple scales. Earth Surf. Process. Landforms 40, 177–188. https://doi.org/10.1002/esp.3635.

Brierley, G., Fryirs, K., Jain, V., 2006. Landscape connectivity: the geographic basis of geomorphic applications. Area 38, 165–174. https://doi.org/10.1111/j.1475-4762.2006.00671.x.

Calsamiglia, A., Fortesa, J., García-Comendador, J., Lucas-Borja, M.E., Calvo-Cases, A., Estrany, J., 2018. Spatial patterns of sediment connectivity in terraced lands: Anthropogenic controls of catchment sensitivity. L. Degrad. Dev. 29, 1198–1210. https://doi.org/10.1002/ldr.2840.

Cantreul, V., Bielders, C., Calsamiglia, A., Degré, A., 2018. How pixel size affects a sediment connectivity index in Central Belgium. Earth Surf. Process. Landforms 43, 884–893. https://doi.org/10.1002/esp.4295.

Cavalli, M., Trevisani, S., Comiti, F., Marchi, L., 2013. Geomorphometric assessment of spatial sediment connectivity in small Alpine catchments. Geomorphology 188, 31–41. https://doi.org/10.1016/j.geomorph.2012.05.007.

Centeri, C., Barta, K., Jakab, G., Szalai, Z., Bíró, Z., 2009. Comparison of EUROSEM, WEPP, and MEDRUSH model calculations with measured runoff and soil-loss data from rainfall simulations in Hungary. J. Plant Nutr. Soil Sci. 172, 789–797. https://doi.org/10.1002/jpln.200900009.

Cerdan, O., Le Bissonnais, Y., Couturier, A., Saby, N., 2002a. Modelling interrill erosion in small cultivated catchments. Hydrol. Process. 16, 3215–3226. https://doi.org/10.1002/hyp.1098.

Cerdan, O., Souchère, V., Lecomte, V., Couturier, A., Le Bissonnais, Y., 2002b. Incorporating soil surface crusting processes in an expert-based runoff model: sealing and transfer by Runoff and Erosion related to Agricultural Management. CATENA 46, 189–205. https://doi.org/10.1016/S0341-8162(01)00166-7.

Ciampalini, R., Follain, S., Le Bissonnais, Y., 2012. Land soil: a model for analysing the impact of erosion on agricultural landscape evolution. Geomorphology 175–176, 25–37. https://doi.org/10.1016/j.geomorph.2012.06.014.

Clarke, R.T., 1973. A review of some mathematical models used in hydrology, with observations on their calibration and use. J. Hydrol. 19, 1–20. https://doi.org/10.1016/0022-1694(73)90089-9.

Cochrane, T.A., Flanagan, D.C., 2005. Effect of DEM resolutions in the runoff and soil loss predictions of the WEPP watershed model. Trans. ASAE 48, 109–120. https://doi.org/10.13031/2013.17953.

Cossart, É., Fressard, M., 2017. Assessment of structural sediment connectivity within catchments: insights from graph theory. Earth Surf. Dyn. 5, 253–268. https://doi.org/10.5194/esurf-5-253-2017.

Cossart, E., Viel, V., Lissak, C., Reulier, R., Fressard, M., Delahaye, D., 2018. How might sediment connectivity change in space and time? L. Degrad. Dev. 29, 2595–2613. https://doi.org/10.1002/ldr.3022.

Coulthard, T.J., Van De Wiel, M.J., 2017. Modelling long term basin scale sediment connectivity, driven by spatial land use changes. Geomorphology 277, 265–281. https://doi.org/10.1016/j.geomorph.2016.05.027.

Crema, S., Cavalli, M., 2018. SedInConnect: a stand-alone, free and open source tool for the assessment of sediment connectivity. Comput. Geosci. 111, 39–45. h10.1016/j.cageo.2017.10.009

Croke, J., Mockler, S., Fogarty, P., Takken, I., 2005. Sediment concentration changes in runoff pathways from a forest road network and the resultant spatial pattern of catchment connectivity. Geomorphology 68, 257–268. https://doi.org/10.1016/j.geomorph.2004.11.020.

Darboux, F., Davy, P., Gascuel-Odoux, C., Huang, C., 2002. Evolution of soil surface roughness and flowpath connectivity in overland flow experiments. CATENA 46, 125–139. https://doi.org/10.1016/S0341-8162(01)00162-X.

David, M., Follain, S., Ciampalini, R., Le Bissonnais, Y., Couturier, A., Walter, C., 2014. Simulation of medium-term soil redistributions for different land use and landscape design scenarios within a vineyard landscape in Mediterranean France. Geomorphology 214, 10–21. https://doi.org/10.1016/j.geomorph.2014.03.016.

De Roo, A.P.J., Jetten, V.G., 1999. Calibrating and validating the LISEM model for two data sets from the Netherlands and South Africa. CATENA 37, 477–493. https://doi.org/10.1016/S0341-8162(99)00034-X.

De Roo, A.P.J., Offermans, R.J.E., Cremers, N.H.D.T., 1996a. Lisem: a single-event, physically based hydrological and soil erosion model for drainage basins. II: sensitivity analysis, validation and application. Hydrol. Process. 10, 1119–1126. https://doi.org/10.1002/(SICI)1099-1085(199608)10:8<1119::AID-HYP416>3.0.CO;2-V.

De Roo, A.P.J., Wesseling, C.G., Ritsema, C.J., 1996b. Lisem: a single-event physically based hydrological and soil erosion model for drainage basins. I: theory, input and output. Hydrol. Process. 10, 1107–1117. https://doi.org/10.1002/(SICI)1099-1085(199608)10:8<1107::AID-HYP415>3.0.CO;2-4.

de Walque, B., Degré, A., Maugnard, A., Bielders, C.L., 2017. Artificial surfaces characteristics and sediment connectivity explain muddy flood hazard in Wallonia. CATENA 158, 89–101. https://doi.org/10.1016/j.catena.2017.06.016.

Delestre, O., Lucas, C., Ksinant, P.-A., Darboux, F., Laguerre, C., Vo, T.-N.-T., James, F., Cordier, S., 2013. SWASHES: a compilation of shallow water analytic solutions for hydraulic and environmental studies. Int. J. Numer. Methods Fluids 72, 269–300. https://doi.org/10.1002/fld.3741.

Delestre, O., Darboux, F., James, F., Lucas, C., Laguerre, C., Cordier, S., 2017. FullSWOF: Full Shallow-Water equations for Overland Flow. J. Open Source Softw. 2, 448.

Estrany, J., Ruiz, M., Calsamiglia, A., Carriquí, M., García-Comendador, J., Nadal, M., Fortesa, J., López-Tarazón, J.A., Medrano, H., Gago, J., 2019. Sediment connectivity linked to vegetation using UAVs: high-resolution imagery for ecosystem management. Sci. Total Environ. 671, 1192–1205. https://doi.org/10.1016/j.scitotenv.2019.03.399.

Evrard, O., Bielders, C.L., Vandaele, K., van Wesemael, B., 2007. Spatial and temporal variation of muddy floods in central Belgium, off-site impacts and potential control measures. CATENA 70, 443–454. https://doi.org/10.1016/j.catena.2006.11.011.

Evrard, O., Cerdan, O., van Wesemael, B., Chauvet, M., Le Bissonnais, Y., Raclot, D., Vandaele, K., Andrieux, P., Bielders, C., 2009. Reliability of an expert-based runoff and erosion model: application of STREAM to different environments. CATENA 78, 129–141. https://doi.org/10.1016/j.catena.2009.03.009.

Favis-Mortlock, D.T., Boardman, J., Parsons, A.J., Lascelles, B., 2000. Emergence and erosion: a model for rill initiation and development. Hydrol. Process. 14, 2173–2205. https://doi.org/10.1002/1099-1085(20000815/30)14:11/12<2173::AID-HYP61>3.0.CO;2-6.

Fiener, P., Wilken, F., Auerswald, K., 2019. Filling the gap between plot and landscape scale – eight years of soil erosion monitoring in 14 adjacent watersheds under soil conservation at Scheyern, Southern Germany. Adv. Geosci. 48, 31–48. https://doi.org/10.5194/adgeo-48-31-2019.

Follain, S., Ciampalini, R., Crabit, A., Coulouma, G., Garnier, F., 2012. Effects of redistribution processes on rock fragment variability within a vineyard topsoil in Mediterranean France. Geomorphology 175–176, 45–53. https://doi.org/10.1016/j.geomorph.2012.06.017.

Foster, G., Meyer, L., 1975. Mathematical simulation of upland erosion by fundamental erosion mechanics. Present and prospective technology for predicting sediment yields and sources. Proceedings of the Sediment-yield Workshop, USDA Sedimentation Laboratory, Oxford, Mississippi, USA.

Freeze, R.A., Harlan, R.L., 1969. Blueprint for a physically-based, digitally-simulated hydrologic response model. J. Hydrol. 9, 237–258. https://doi.org/10.1016/0022-1694(69)90020-1.

Fryirs, K., 2013. (Dis)Connectivity in catchment sediment cascades: a fresh look at the sediment delivery problem. Earth Surf. Process. Landforms 38, 30–46. https://doi.org/10.1002/esp.3242.

Fryirs, K.A., Brierley, G.J., Preston, N.J., Kasai, M., 2007. Buffers, barriers and blankets: the (dis)connectivity of catchment-scale sediment cascades. CATENA 70, 49–67. https://doi.org/10.1016/j.catena.2006.07.007.

Gay, A., Cerdan, O., Mardhel, V., Desmet, M., 2016. Application of an index of sediment connectivity in a lowland area. J. Soils Sediments 16, 280–293. https://doi.org/10.1007/s11368-015-1235-y.

Gerwin, W., Schaaf, W., Biemelt, D., Fischer, A., Winter, S., Hüttl, R.F., 2009. The artificial catchment "Chicken Creek" (Lusatia, Germany)—a landscape laboratory for interdisciplinary studies of initial ecosystem development. Ecol. Eng. 35, 1786–1796. https://doi.org/10.1016/j.ecoleng.2009.09.003.

GISER, 2011. Convention GISER (Rapport final).

Govers, G., Vandaele, K., Desmet, P., Poesen, J., Bunte, K., 1994. The role of tillage in soil redistribution on hillslopes. Eur. J. Soil Sci. 45, 469–478. https://doi.org/10.1111/j.1365-2389.1994.tb00532.x.

Grum, B., Woldearegay, K., Hessel, R., Baartman, J.E.M., Abdulkadir, M., Yazew, E., Kessler, A., Ritsema, C.J., Geissen, V., 2017. Assessing the effect of water harvesting techniques on event-based hydrological responses and sediment yield at a catchment scale in northern Ethiopia using the Limburg Soil Erosion Model (LISEM). CATENA 159, 20–34. https://doi.org/10.1016/j.catena.2017.07.018.

Gumiere, S.J., Le Bissonnais, Y., Raclot, D., Cheviron, B., 2011. Vegetated filter effects on sedimentological connectivity of agricultural catchments in erosion modelling: a review. Earth Surf. Process. Landforms 36, 3–19. https://doi.org/10.1002/esp.2042.

Hartley, D.M., Julien, P.Y., 1992. Boundary shear stress induced by raindrop impact. J. Hydraul. Res. 30, 341–359. https://doi.org/10.1080/00221689209498923.

Heckmann, T., Schwanghart, W., 2013. Geomorphic coupling and sediment connectivity in an alpine catchment — exploring sediment cascades using graph theory. Geomorphology 182, 89–103. https://doi.org/10.1016/j.geomorph.2012.10.033.

Heckmann, T., Cavalli, M., Cerdan, O., Foerster, S., Javaux, M., Lode, E., Smetanová, A., Vericat, D., Brardinoni, F., 2018. Indices of sediment connectivity: opportunities, challenges and limitations. Earth-Science Rev. 187, 77–108. https://doi.org/10.1016/j.earscirev.2018.08.004.

Hessel, R., 2005. Effects of grid cell size and time step length on simulation results of the Limburg soil erosion model (LISEM). Hydrol. Process. 19, 3037–3049. https://doi.org/10.1002/hyp.5815.

Hessel, R., Jetten, V., Liu, B., Zhang, Y., Stolte, J., 2003. Calibration of the LISEM model for a small Loess Plateau catchment. CATENA 54, 235–254. https://doi.org/10.1016/S0341-8162(03)00067-5.

Hong, Y., Bonhomme, C., Le, M.-H., Chebbo, G., 2016. A new approach of monitoring and physically-based modelling to investigate urban wash-off process on a road catchment near Paris. Water Res. 102, 96–108. https://doi.org/10.1016/j.watres.2016.06.027.

Hutchinson, M.F., Xu, T., Stein, J.A., 2011. Recent progress in the ANUDEM elevation gridding procedure. In: Hengl, T., Evans, I.~S., Wilson, J.~P., Gould, M. (Eds.), Geomorphometry. 2011, pp. 19–22 (Redlands, CA).

Jetten, V., de Roo, A., Favis-Mortlock, D., 1999. Evaluation of field-scale and catchment-scale soil erosion models. CATENA 37, 521–541. https://doi.org/10.1016/S0341-8162(99)00037-5.

Jetten, V., Govers, G., Hessel, R., 2003. Erosion models: quality of spatial predictions. Hydrol. Process. 17, 887–900. https://doi.org/10.1002/hyp.1168.

Kalantari, Z., Ferreira, C.S.S., Koutsouris, A.J., Ahlmer, A.-K., Cerdà, A., Destouni, G., 2019. Assessing flood probability for transportation infrastructure based on catchment characteristics, sediment connectivity and remotely sensed soil moisture. Sci. Total Environ. 661, 393–406. https://doi.org/10.1016/j.scitotenv.2019.01.009.

Karamesouti, M., Petropoulos, G.P., Papanikolaou, I.D., Kairis, O., Kosmas, K., 2016. Erosion rate predictions from PESERA and RUSLE at a Mediterranean site before and after a wildfire: comparison & implications. Geoderma 261, 44–58. https://doi.org/10.1016/j.geoderma.2015.06.025.

Keesstra, S., Nunes, J.P., Saco, P., Parsons, T., Poeppl, R., Masselink, R., Cerdà, A., 2018. The way forward: can connectivity be useful to design better measuring and modelling schemes for water and sediment dynamics? Sci. Total Environ. 644, 1557–1572. https://doi.org/10.1016/j.scitotenv.2018.06.342.

Kinnell, P.I.A., 2017. A comparison of the abilities of the USLE-M, RUSLE2 and WEPP to model event erosion from bare fallow areas. Sci. Total Environ. 596–597, 32–42. https://doi.org/10.1016/j.scitotenv.2017.04.046.

Kirkby, M., 1971. Hillslope process-response models based on the continuity equation. Trans. Inst. Br. Geogr. 3, 15–30.

Kværnø, S.H., Stolte, J., 2012. Effects of soil physical data sources on discharge and soil loss simulated by the LISEM model. CATENA 97, 137–149. https://doi.org/10.1016/j.catena.2012.05.001.

Laloy, E., 2010. Measuring and Modeling the Impact of Intercrop Management on Plot-scale Runoff and Erosion in a Continuous Maize Cropping System. Université catholique de Louvain.

Laloy, E., Bielders, C.L., 2008. Plot scale continuous modelling of runoff in a maize cropping system with dynamic soil surface properties. J. Hydrol. 349, 455–469. https://doi.org/10.1016/j.jhydrol.2007.11.033.

Landemaine, V., 2016. Érosion des sols et transferts sédimentaires sur les bassins versants de l'Ouest du Bassin de Paris : analyse, quantification et modélisation à l'échelle pluriannuelle.

Le Bissonnais, Y., Benkhadra, H., Chaplot, V., Fox, D., King, D., Daroussin, J., 1998. Crusting, runoff and sheet erosion on silty loamy soils at various scales and upscaling from m2 to small catchments. Soil Tillage Res. 46, 69–80. https://doi.org/10.1016/S0167-1987(98)80109-8.

Le Bissonnais, Y., Cerdan, O., Lecomte, V., Benkhadra, H., Souchère, V., Martin, P., 2005. Variability of soil surface characteristics influencing runoff and interrill erosion. CATENA 62, 111–124. https://doi.org/10.1016/j.catena.2005.05.001.

Lesschen, J.P., Schoorl, J.M., Cammeraat, L.H., 2009. Modelling runoff and erosion for a semi-arid catchment using a multi-scale approach based on hydrological connectivity. Geomorphology 109, 174–183. https://doi.org/10.1016/j.geomorph.2009.02.030.

Lexartza-Artza, I., Wainwright, J., 2009. Hydrological connectivity: linking concepts with practical implications. CATENA 79, 146–152. https://doi.org/10.1016/j.catena.2009.07.001.

Li, Z., Fang, H., 2016. Impacts of climate change on water erosion: a review. Earth-Science Rev. 163, 94–117. https://doi.org/10.1016/j.earscirev.2016.10.004.

Liu, Y., Fu, B., 2016. Assessing sedimentological connectivity using WATEM/SEDEM model in a hilly and gully watershed of the Loess Plateau, China. Ecol. Indic. 66, 259–268. https://doi.org/10.1016/j.ecolind.2016.01.055.

Llena, M., Vericat, D., Cavalli, M., Crema, S., Smith, M.W., 2019. The effects of land use and topographic changes on sediment connectivity in mountain catchments. Sci. Total Environ. 660, 899–912. https://doi.org/10.1016/j.scitotenv.2018.12.479.

López-Vicente, M., Poesen, J., Navas, A., Gaspar, L., 2013. Predicting runoff and sediment connectivity and soil erosion by water for different land use scenarios in the Spanish Pre-Pyrenees. CATENA 102, 62–73. https://doi.org/10.1016/j.catena.2011.01.001.

López-Vicente, M., Quijano, L., Palazón, L., Gaspar, L., Navas, A., 2015. Assessment of soil redistribution at catchment scale by coupling a soil erosion model and a sediment connectivity index (central spanish pre-pyrenees). Cuad. Investig. Geográfica; Vol 41, No 1 (2015) DO - 10.18172/cig.2649.

López-Vicente, M., Nadal-Romero, E., Cammeraat, E.L.H., 2017. Hydrological connectivity does change over 70years of abandonment and afforestation in the Spanish Pyrenees. L. Degrad. Dev. 28, 1298–1310. https://doi.org/10.1002/ldr.2531.

Mahoney, D.T., Fox, J.F., Al Aamery, N., 2018. Watershed erosion modeling using the probability of sediment connectivity in a gently rolling system. J. Hydrol. 561, 862–883. https://doi.org/10.1016/j.jhydrol.2018.04.034.

Martínez-Murillo, J.F., López-Vicente, M., 2018. Effect of salvage logging and check dams on simulated hydrological connectivity in a burned area. L. Degrad. Dev. 29, 701–712. https://doi.org/10.1002/ldr.2735.

Masselink, R.J.H., Keesstra, S.D., Temme, A.J.A.M., Seeger, M., Giménez, R., Casalí, J., 2016. Modelling discharge and sediment yield at catchment scale using connectivity components. L. Degrad. Dev. 27, 933–945. https://doi.org/10.1002/ldr.2512.

Masselink, R.J.H., Heckmann, T., Temme, A.J.A.M., Anders, N.S., Gooren, H.P.A., Keesstra, S.D., 2017. A network theory approach for a better understanding of overland flow connectivity. Hydrol. Process. 31, 207–220. https://doi.org/10.1002/hyp.10993.

Maugnard, A., 2015. Characterization and Prediction of Ephemeral Gully Erosion in Wallonia. Université catholique de Louvain.

Maugnard, A., Bielders, C.L., Bock, L., Colinet, G., Cordonnier, H., Degré, A., Demarcin, P., Dewez, A., Feltz, N., Legrain, X., Pineux, N., Mokadem, A.I., 2013. Cartographie du risque d'érosion hydrique a l'échelle parcellaire en soutien a la politique agricole wallonne (Belgique). Étude Gest. des Sols 20, 127–141.

Mekonnen, M., Keesstra, S.D., Ritsema, C.J., Stroosnijder, L., Baartman, J.E.M., 2016. Sediment trapping with indigenous grass species showing differences in plant traits in Northwest Ethiopia. CATENA 147, 755–763. https://doi.org/10.1016/j.catena.2016.08.036.

Mora, J.L., Lázaro, R., 2013. Evidence of a threshold in soil erodibility generating differences in vegetation development and resilience between two semiarid grasslands. J. Arid Environ. 89, 57–66. https://doi.org/10.1016/j.jaridenv.2012.10.005.

Morgan, R.P.C., 2001. A simple approach to soil loss prediction: a revised Morgan–Morgan–Finney model. CATENA 44, 305–322. https://doi.org/10.1016/S0341-8162(00)00171-5.

Mueller, E.N., Wainwright, J., Parsons, A.J., 2007. Impact of connectivity on the modeling of overland flow within semiarid shrubland environments. Water Resour. Res. 43. https://doi.org/10.1029/2006WR005006.

Nearing, M.A., 1998. Why soil erosion models over-predict small soil losses and under-predict large soil losses. CATENA 32, 15–22. https://doi.org/10.1016/S0341-8162(97)00052-0.

Nearing, M.A., 2000. Evaluating soil erosion models using measured plot data: accounting for variability in the data. Earth Surf. Process. Landforms 25, 1035–1043. https://doi.org/10.1002/1096-9837(200008)25:9<1035::AID-ESP121>3.0.CO;2-B.

Nearing, M.A., Lane, L.J., Alberts, E.E., Laflen, J.M., 1990. Prediction technology for soil erosion by water: status and research needs. Soil Sci. Soc. Am. J. 54, 1702–1711. https://doi.org/10.2136/sssaj1990.03615995005400060033x.
Nearing, M.A., Jetten, V., Baffaut, C., Cerdan, O., Couturier, A., Hernandez, M., Le Bissonnais, Y., Nichols, M.H., Nunes, J.P., Renschler, C.S., Souchère, V., van Oost, K., 2005. Modeling response of soil erosion and runoff to changes in precipitation and cover. CATENA 61, 131–154. https://doi.org/10.1016/j.catena.2005.03.007.
Nunes, J.P., Vieira, G.N., Seixas, J., Gonçalves, P., Carvalhais, N., 2005. Evaluating the MEFIDIS model for runoff and soil erosion prediction during rainfall events. CATENA 61, 210–228. https://doi.org/10.1016/j.catena.2005.03.005.
Nunes, J.P., de Lima, J.L.M.P., Singh, V.P., de Lima, M.I.P., Vieira, G.N., 2006. Numerical modeling of surface runoff and erosion due to moving rainstorms at the drainage basin scale. J. Hydrol. 330, 709–720. https://doi.org/10.1016/j.jhydrol.2006.04.037.
Nunes, J.P., Seixas, J., Keizer, J.J., Ferreira, A.J.D., 2009. Sensitivity of runoff and soil erosion to climate change in two Mediterranean watersheds. Part II: assessing impacts from changes in storm rainfall, soil moisture and vegetation cover. Hydrol. Process. 23, 1212–1220. https://doi.org/10.1002/hyp.7250.
Nunes, J.P., Wainwright, J., Bielders, C.L., Darboux, F., Fiener, P., Finger, D., Turnbull, L., 2018. Better models are more effectively connected models. Earth Surf. Process. Landforms 43, 1355–1360. https://doi.org/10.1002/esp.4323.
Parsons, A.J., Bracken, L., Poeppl, R.E., Wainwright, J., Keesstra, S.D., 2015. Introduction to special issue on connectivity in water and sediment dynamics. Earth Surf. Process. Landforms 40, 1275–1277. https://doi.org/10.1002/esp.3714.
Peñuela, A., Darboux, F., Javaux, M., Bielders, C., 2016. Evolution of overland flow connectivity in bare agricultural plots. Earth Surf. Process. Landf. 41, 1595–1613. https://doi.org/10.1002/esp.3938.
Persichillo, M.G., Bordoni, M., Cavalli, M., Crema, S., Meisina, C., 2018. The role of human activities on sediment connectivity of shallow landslides. CATENA 160, 261–274. https://doi.org/10.1016/j.catena.2017.09.025.
Pineux, N., Michel, B., Legrain, X., Bielders, C.L., Degré, A., Colinet, G., 2017. Diachronic soil surveys: a method for quantifying long-term diffuse erosion? Geoderma Reg. 10, 102–114. https://doi.org/10.1016/j.geodrs.2017.06.001.
Planchon, O., Darboux, F., 2002. A fast, simple and versatile algorithm to fill the depressions of digital elevation models. CATENA 46, 159–176. https://doi.org/10.1016/S0341-8162(01)00164-3.
Poeppl, R.E., Keiler, M., Von Elverfeldt, K., Zweimueller, I., Glade, T., 2012. The influence of riparian vegetation cover on diffuse lateral sediment connectivity and biogeomorphic processes in a medium-sized agricultural catchment, Austria. Geogr. Ann. Ser. A, Phys. Geogr. 94, 511–529. https://doi.org/10.1111/j.1468-0459.2012.00476.x.
Poeppl, R.E., Keesstra, S.D., Hein, T., 2015. The geomorphic legacy of small dams—an Austrian study. Anthropocene 10, 43–55. https://doi.org/10.1016/j.ancene.2015.09.003.
Poeppl, R.E., Keesstra, S.D., Maroulis, J., 2017. A conceptual connectivity framework for understanding geomorphic change in human-impacted fluvial systems. Geomorphology 277, 237–250. https://doi.org/10.1016/j.geomorph.2016.07.033.
Poeppl, E.R., Dilly, A.L., Haselberger, S., Renschler, S.C., Baartman, E.M.J., 2019. Combining soil erosion modeling with connectivity analyses to assess lateral fine sediment input into agricultural streams. Water. https://doi.org/10.3390/w11091793.
Renschler, C.S., 2003. Designing geo-spatial interfaces to scale process models: the GeoWEPP approach. Hydrol. Process. 17, 1005–1017. https://doi.org/10.1002/hyp.1177.
Reulier, R., Delahaye, D., Viel, V., 2019. Agricultural landscape evolution and structural connectivity to the river for matter flux, a multi-agents simulation approach. CATENA 174, 524–535. https://doi.org/10.1016/j.catena.2018.11.036.
Saco, P.M., Willgoose, G.R., Hancock, G.R., 2007. Eco-geomorphology of banded vegetation patterns in arid and semi-arid regions. Hydrol. Earth Syst. Sci. 11, 1717–1730. https://doi.org/10.5194/hess-11-1717-2007.
Schindewolf, M., Schmidt, J., 2012. Parameterization of the EROSION 2D/3D soil erosion model using a small-scale rainfall simulator and upstream runoff simulation. CATENA 91, 47–55. https://doi.org/10.1016/j.catena.2011.01.007.
Schmidt, J., 1991. A mathematical model to simulate rainfall erosion. Catena Suppl. 19, 101–109.
Schmidt, J., 1996. Entwicklung und Anwendung eines physikalisch begründeten Simulationsmodells für die Erosion geneigter landwirtschaftlicher Nutzflächen. Selbstverl. des Inst. für Geograph. Wiss, Berlin.
Service public de Wallonie, 2005. ERUISSOL, DEM.
Shen, Z.Y., Gong, Y.W., Li, Y.H., Hong, Q., Xu, L., Liu, R.M., 2009. A comparison of WEPP and SWAT for modeling soil erosion of the Zhangjiachong Watershed in the Three Gorges Reservoir Area. Agric. Water Manag. 96, 1435–1442. https://doi.org/10.1016/j.agwat.2009.04.017.
Smetanová, A., Paton, E.N., Maynard, C., Tindale, S., Fernández-Getino, A.P., Marqéus Pérez, M.J., Bracken, L., Le Bissonnais, Y., Keesstra, S.D., 2018. Stakeholders' perception of the relevance of water and sediment connectivity in water and land management. L. Degrad. Dev. 29, 1833–1844. https://doi.org/10.1002/ldr.2934.
Smith, R.E., Goodrich, D.C., Quinton, J.N., 1995. Dynamic, distributed simulation of watershed erosion: the KINEROS2 and EUROSEM models. J. Soil Water Conserv. 50, 517–520.
Souchere, V., King, D., Daroussin, J., Papy, F., Capillon, A., 1998. Effects of tillage on runoff directions: consequences on runoff contributing area within agricultural catchments. J. Hydrol. 206, 256–267. https://doi.org/10.1016/S0022-1694(98)00103-6.
Souchere, V., Cerdan, O., Ludwig, B., Le Bissonnais, Y., Couturier, A., Papy, F., 2003. Modelling ephemeral gully erosion in small cultivated catchments. CATENA 50, 489–505. https://doi.org/10.1016/S0341-8162(02)00124-8.
Starkloff, T., Stolte, J., 2014. Applied comparison of the erosion risk models EROSION 3D and LISEM for a small catchment in Norway. CATENA 118, 154–167. https://doi.org/10.1016/j.catena.2014.02.004.
Starkloff, T., Stolte, J., Hessel, R., Ritsema, C., Jetten, V., 2018. Integrated, spatial distributed modelling of surface runoff and soil erosion during winter and spring. CATENA 166, 147–157. https://doi.org/10.1016/j.catena.2018.04.001.
Takken, I., Beuselinck, L., Nachtergaele, J., Govers, G., Poesen, J., Degraer, G., 1999. Spatial evaluation of a physically-based distributed erosion model (LISEM). CATENA 37, 431–447. https://doi.org/10.1016/S0341-8162(99)00031-4.
Takken, I., Govers, G., Jetten, V., Nachtergaele, J., Steegen, A., Poesen, J., 2005. The influence of both process descriptions and runoff patterns on predictions from a spatially distributed soil erosion model. Earth Surf. Process. Landforms 30, 213–229. https://doi.org/10.1002/esp.1176.
Tan, Z., Leung, L.R., Li, H.-Y., Tesfa, T., 2018. Modeling sediment yield in land surface and earth system models: model comparison, development, and evaluation. J. Adv. Model. Earth Syst. 10, 2192–2213. https://doi.org/10.1029/2017MS001270.
Tavares Wahren, F., Julich, S., Nunes, J.P., Gonzalez-Pelayo, O., Hawtree, D., Feger, K.-H., Keizer, J.J., 2016. Combining digital soil mapping and hydrological modeling in a data scarce watershed in north-central Portugal. Geoderma 264, 350–362. https://doi.org/10.1016/j.geoderma.2015.08.023.
Turnbull, L., Wainwright, J., Brazier, R.E., 2008. A conceptual framework for understanding semi-arid land degradation: ecohydrological interactions across multiple-space and time scales. Ecohydrology 1, 23–34. https://doi.org/10.1002/eco.4.
van der Ploeg, M.J., Baartman, J.E.M., Robinson, D.A., 2018. Biophysical landscape interactions: bridging disciplines and scale with connectivity. L. Degrad. Dev. 29, 1167–1175. https://doi.org/10.1002/ldr.2820.
Van Eck, C.M., Nunes, J.P., Vieira, D.C.S., Keesstra, S., Keizer, J.J., 2016. Physically-based modelling of the post-fire runoff response of a forest catchment in Central Portugal: using field versus remote sensing based estimates of vegetation recovery. L. Degrad. Dev. 27, 1535–1544. https://doi.org/10.1002/ldr.2507.
Vieira, D.C.S., Serpa, D., Nunes, J.P.C., Prats, S.A., Neves, R., Keizer, J.J., 2018. Predicting the effectiveness of different mulching techniques in reducing post-fire runoff and erosion at plot scale with the RUSLE, MMF and PESERA models. Environ. Res. 165, 365–378. https://doi.org/10.1016/j.envres.2018.04.029.
von Werner, M., 1995. GIS-orientierte Methoden der digitalen Reliefanalyse zur Modellierung von Bodenerosion in kleinen Einzugsgebieten.
Wade, C.R., Bolding, M.C., Aust, W.M., Lakel III, W.A., Schilling, E.B., 2012. Comparing sediment trap data with the USLE-forest, RUSLE2, and WEPP-road erosion models for evaluation of bladed skid trail BMPs. Trans. ASABE 55, 403–414. https://doi.org/10.13031/2013.41381.
Wainwright, J., Turnbull, L., Ibrahim, T.G., Lexartza-Artza, I., Thornton, S.F., Brazier, R.E., 2011. Linking environmental régimes, space and time: interpretations of structural and functional connectivity. Geomorphology 126, 387–404. https://doi.org/10.1016/j.geomorph.2010.07.027.
Wilken, F., Sommer, M., Van Oost, K., Bens, O., Fiener, P., 2017. Process-oriented modelling to identify main drivers of erosion-induced carbon fluxes. SOIL 3, 83–94. https://doi.org/10.5194/soil-3-83-2017.
Wittmann, R., Bungartz, H.-J., Neumann, P., 2017. High performance shallow water kernels for parallel overland flow simulations based on FullSWOF2D. Comput. Math. with Appl. 74, 110–125. https://doi.org/10.1016/j.camwa.2017.01.005.
Wohl, E., 2017. Connectivity in rivers. Prog. Phys. Geogr. Earth Environ. 41, 345–362. https://doi.org/10.1177/0309133317714972.
Yang, J., Chu, X., 2013. Quantification of the spatio-temporal variations in hydrologic connectivity of small-scale topographic surfaces under various rainfall conditions. J. Hydrol. 505, 65–77. https://doi.org/10.1016/j.jhydrol.2013.09.013.
Zhang, J.X., Chang, K., Wu, J.Q., 2008. Effects of DEM resolution and source on soil erosion modelling: a case study using the WEPP model. Int. J. Geogr. Inf. Sci. 22, 925–942. https://doi.org/10.1080/13658810701776817.